History of the X-ray brightness

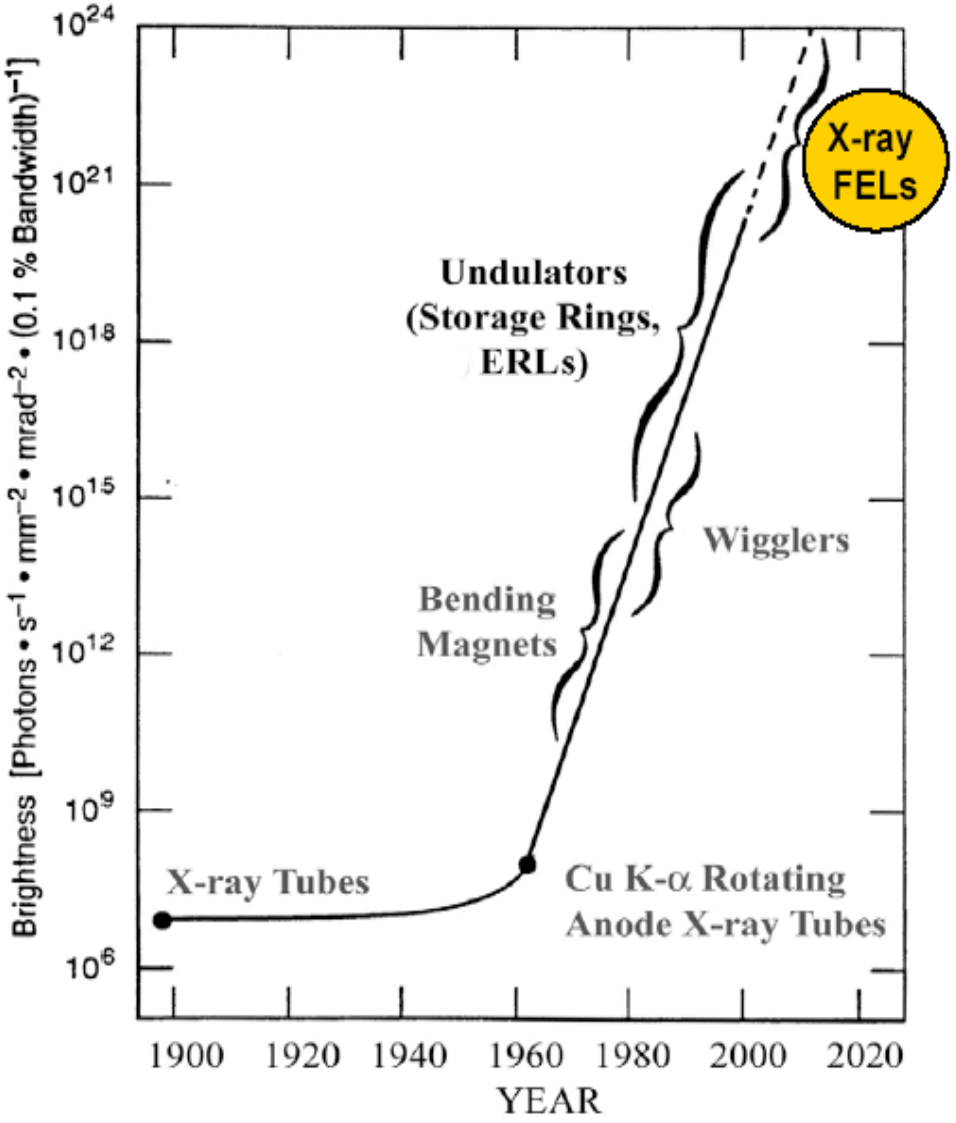

Brighness comparison

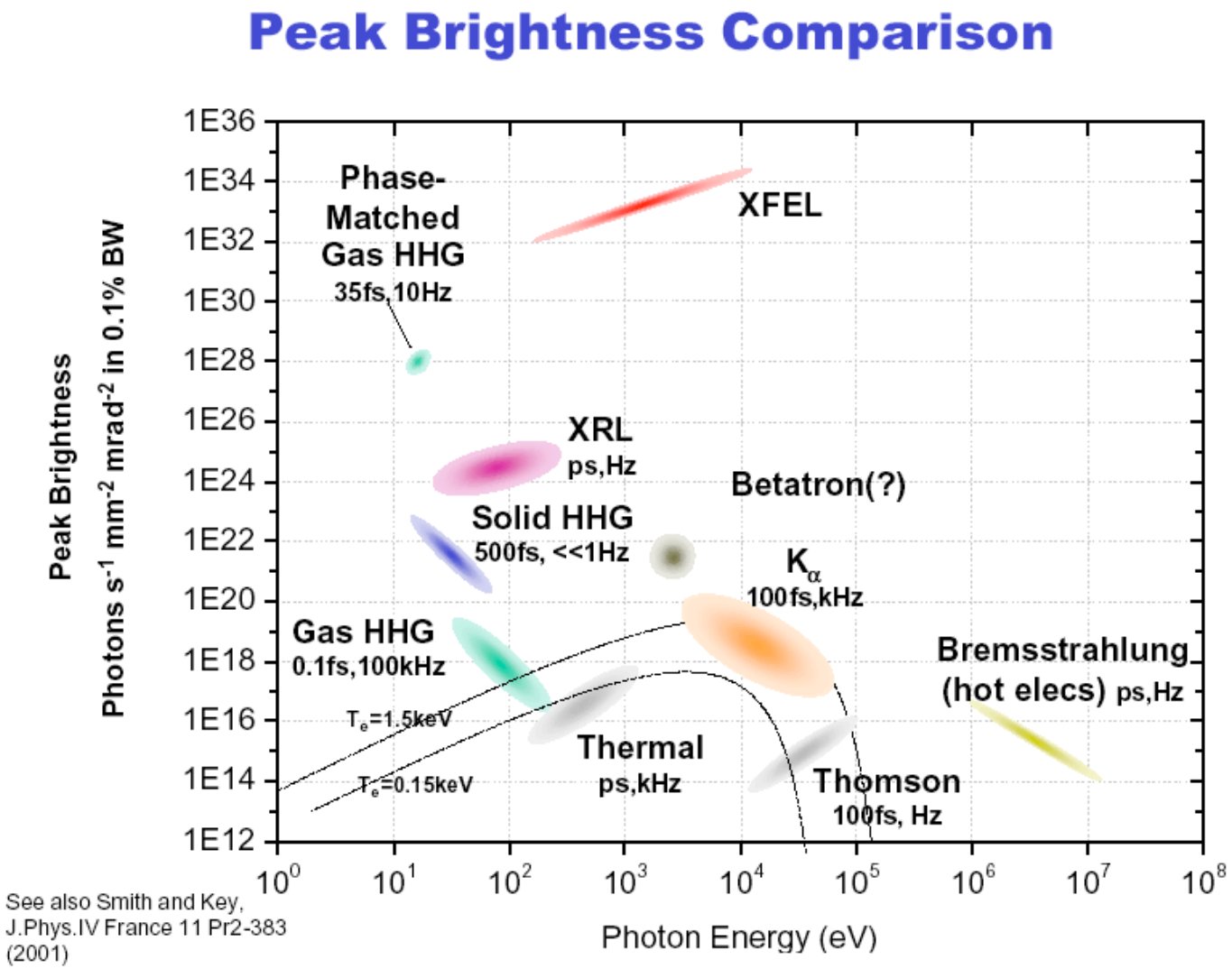

See also Smith and Key, J.Phys.IV France 11 Pr2-383 (2001)

Exploiting the brightness

- Hot Dense Matter occurs in:
  - Supernova, stellar interiors, accretion disks
  - Plasma devices: laser produced plasmas, Z-pinches
  - Directly driven inertial fusion plasma
- Warm Dense Matter occurs in:
  - Cores of large planets
  - Systems that start solid and end as a plasma
  - X-ray driven inertial fusion implosion

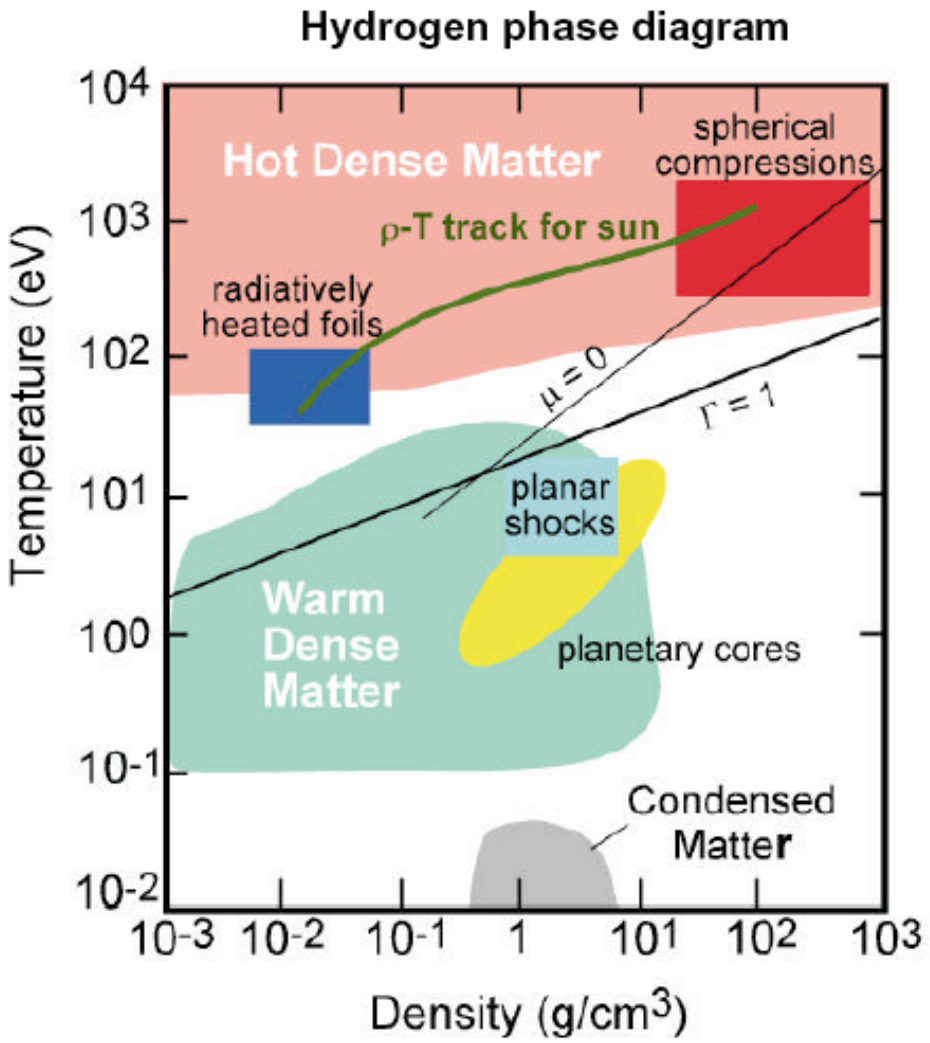

R.W. Lee, LLNL

Processes and time

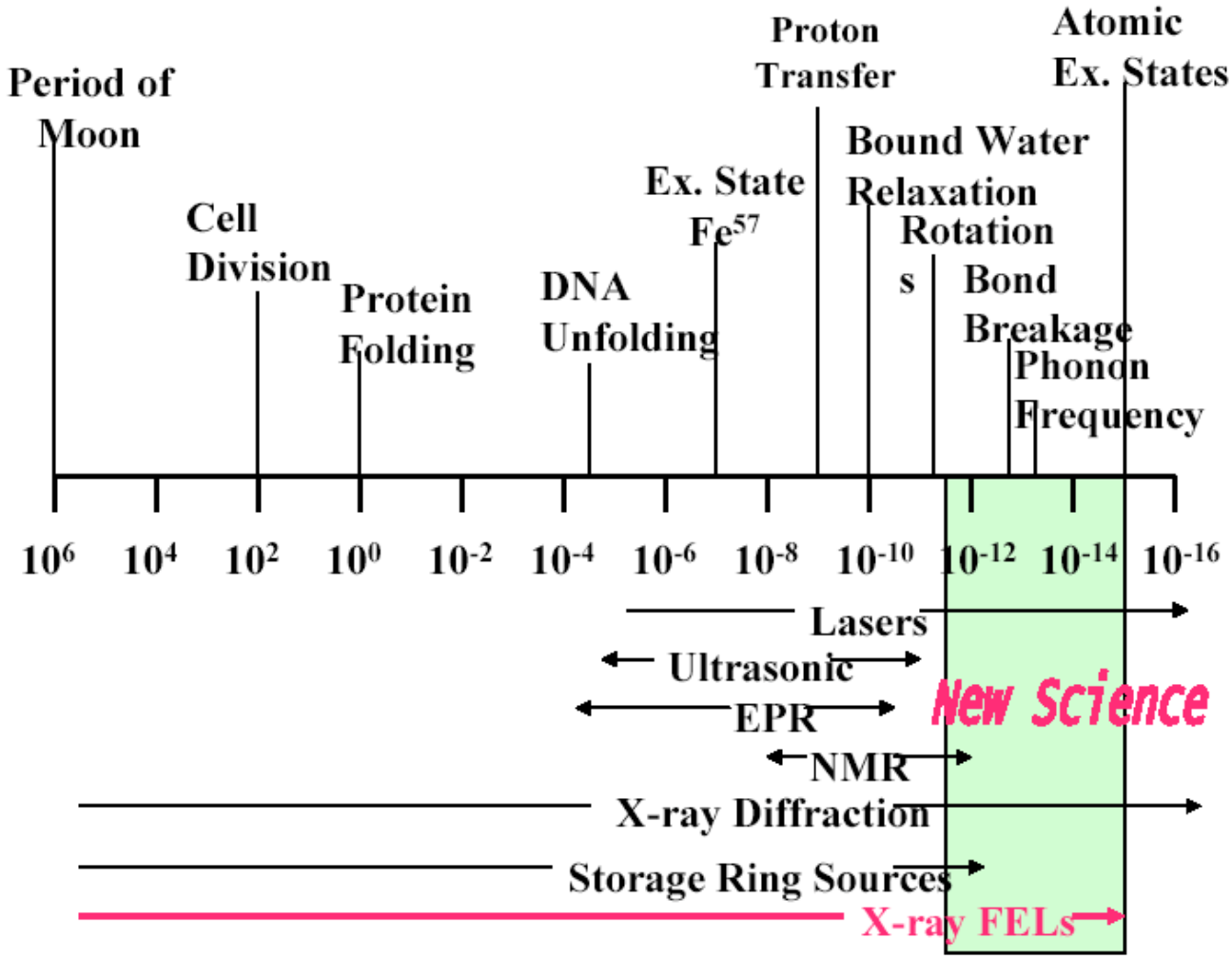

Non-equilibrium dynamics

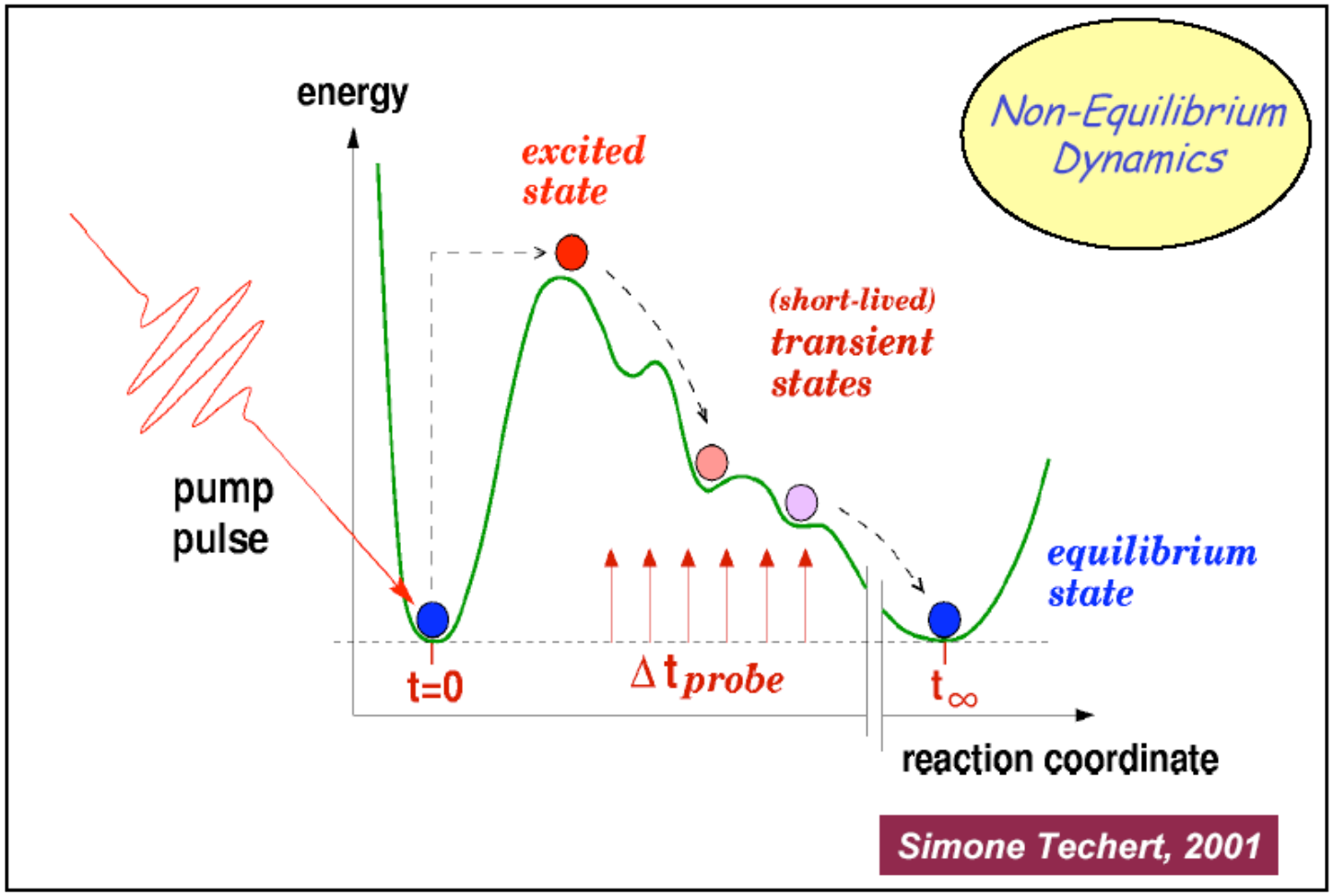

Generation of ultrashort X-ray pulses 1

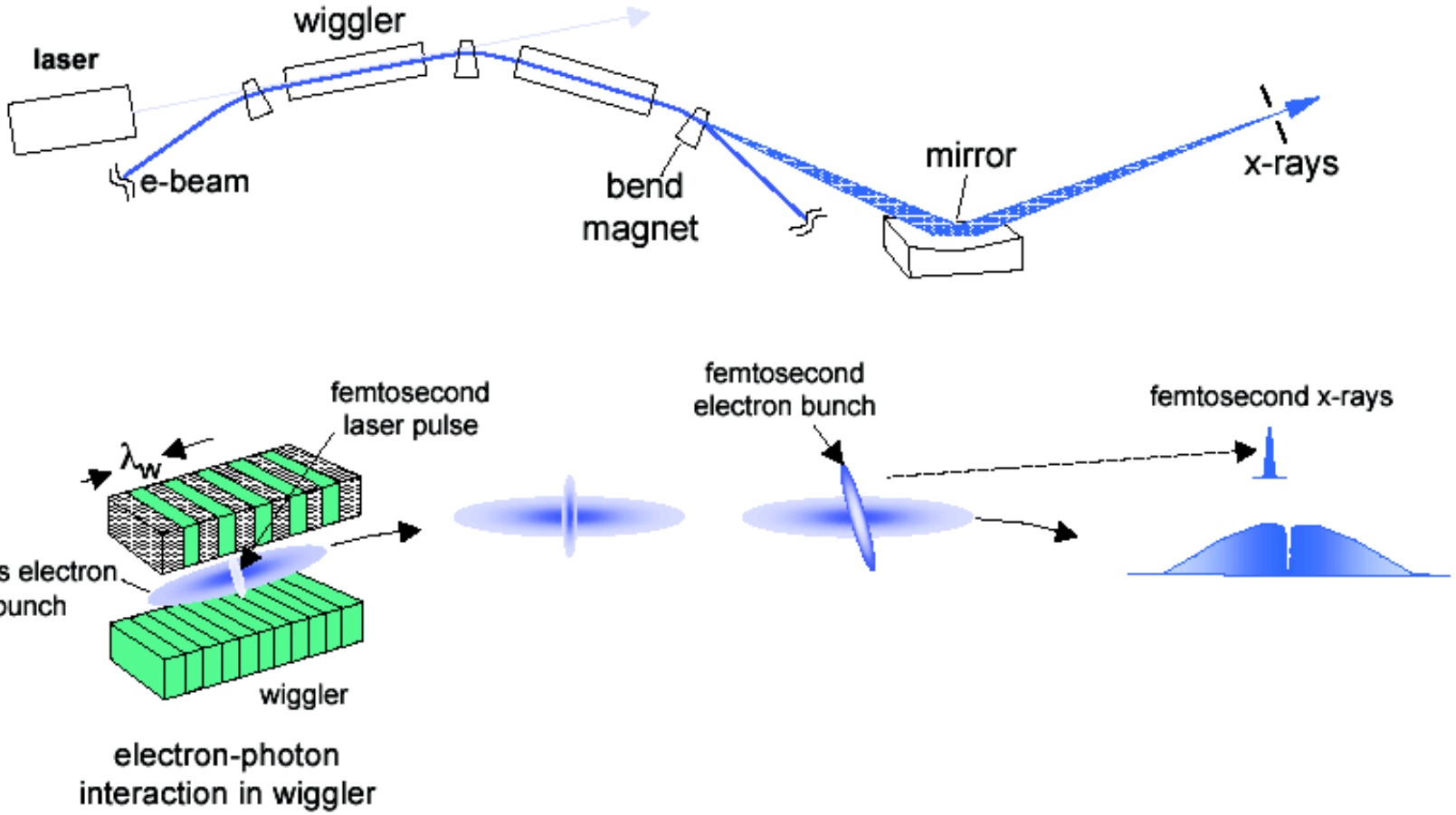

Zholents and Zolotorev, *Phys. Rev. Lett.*, 76, 916,(1996).

Schoenlein et al., *Science*, 287, (2000)

Generation of ultrashort X-ray pulses 2

Klaus Sokolowski-Tinten

Institut für Experimentelle Physik

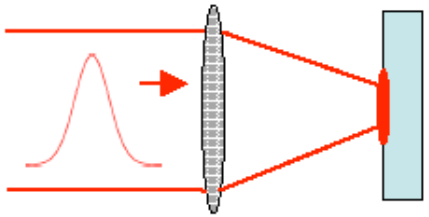

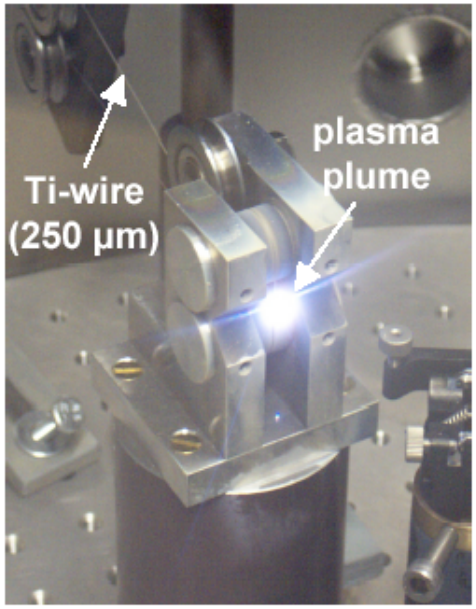

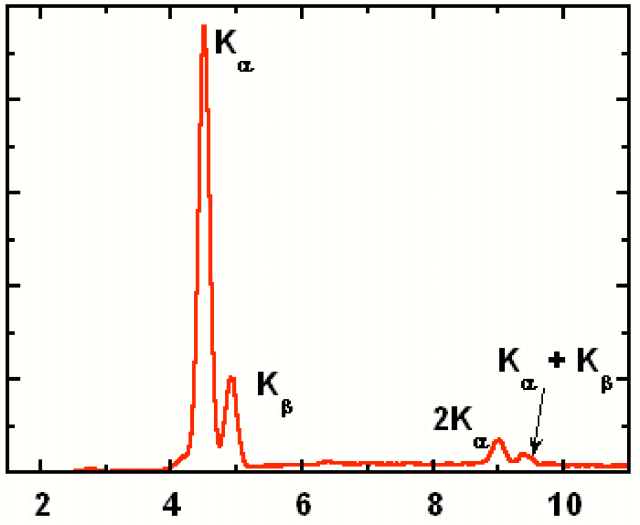

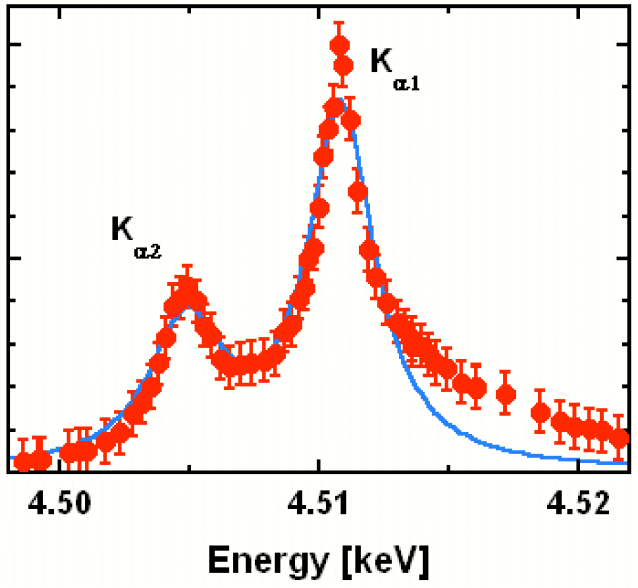

Generation of ultrashort X-ray pulses 3

Klaus Sokolowski-Tinten
Institut für Experimentelle Physik

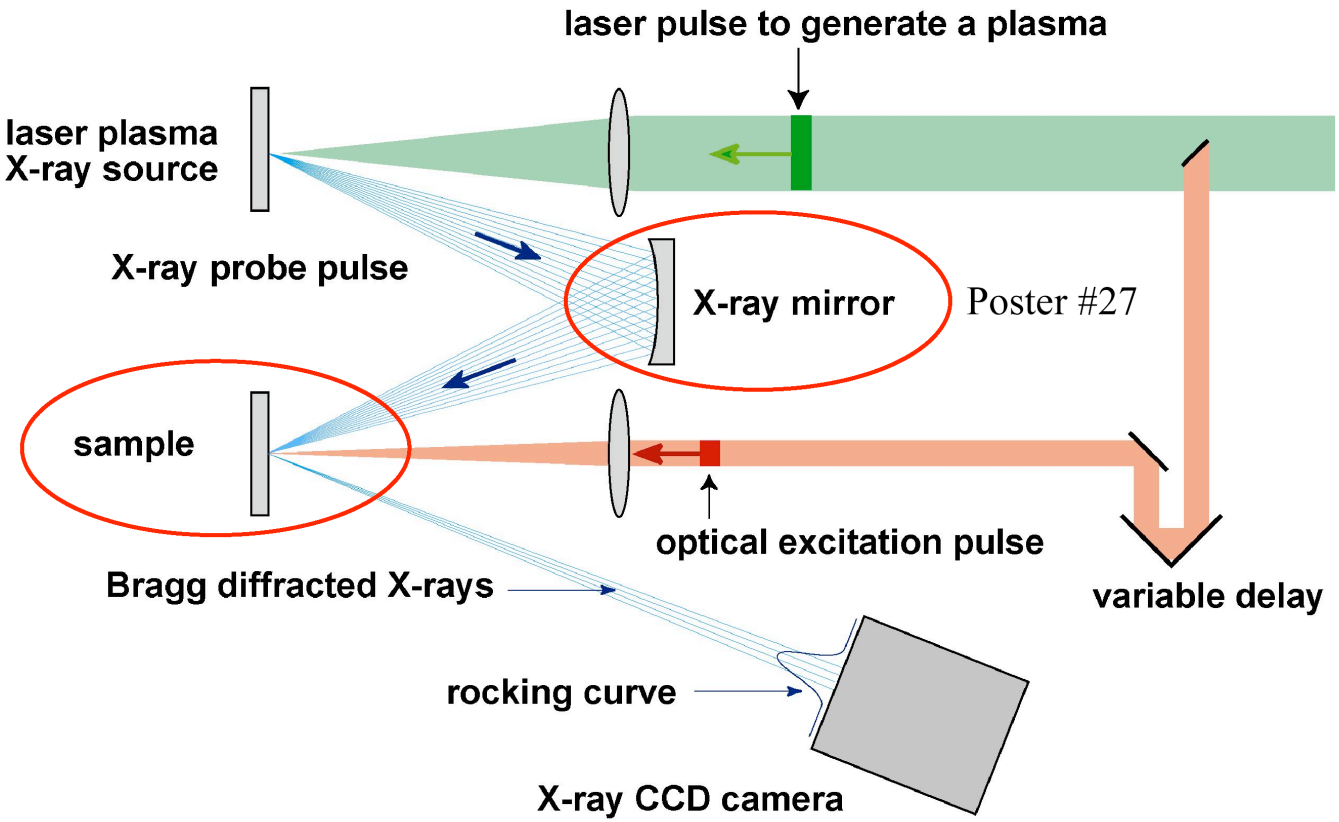

Generation of ultrashort X-ray pulses 5

Max Born Institute
Berlin

Matias Bargheer,
N. Zhavoronkov, Y. Gritsai,
M. Wörner, T. Elsaesser

K_α line radiation:

	K_α energy/ eV	K_α flux / 4π*s
Ga	9.2	4.5×10^{10}
Cu	8.2	3.9×10^{10}
Ni	7.5	6.7×10^{10}

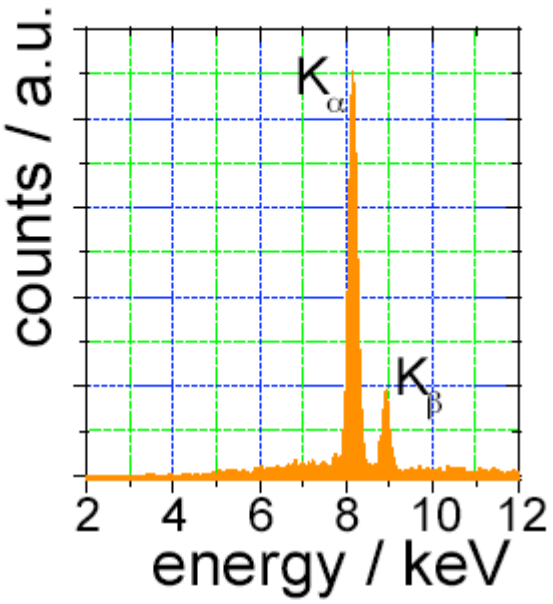

- Plasma generated in 15 μm copper
- X-ray focus 15 μm
- Estimated pulse duration: 200 fs

Brilliance = 4 x 10^7 / (mrad^2*mm^{2}s*0.1%BW)

According to specs	Flux on sample / s	Focus / μm
Multilayer mirror (Osmic)	1.4×10^6	30
HOPG reflector (IfG)	5×10^7	200

Generation of ultrashort X-ray pulses 6

High Harmonic Generation - HHG

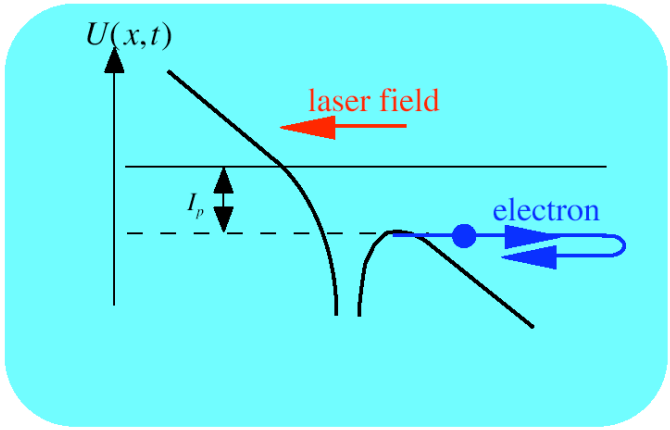

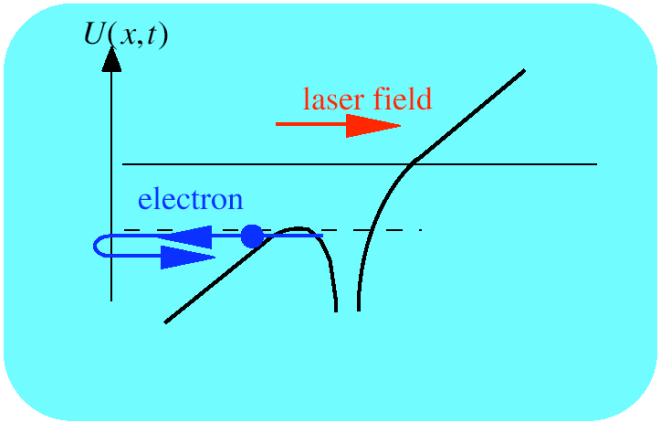

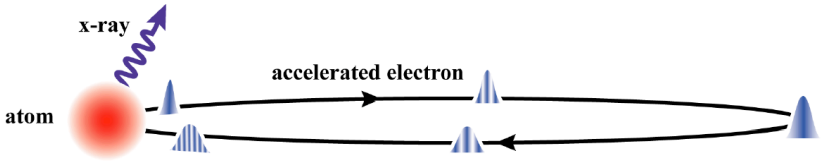

$$\hbar\omega_{cutoff} = I_p + 3.2U_p$$

ionization potential of atom

$U_p \approx I_L \lambda^2$ quiver energy of e⁻

$\varphi_{x\text{-}ray} \approx \varphi_{Laser}$ and I_{Laser}

Generation of ultrashort X-ray pulses 7

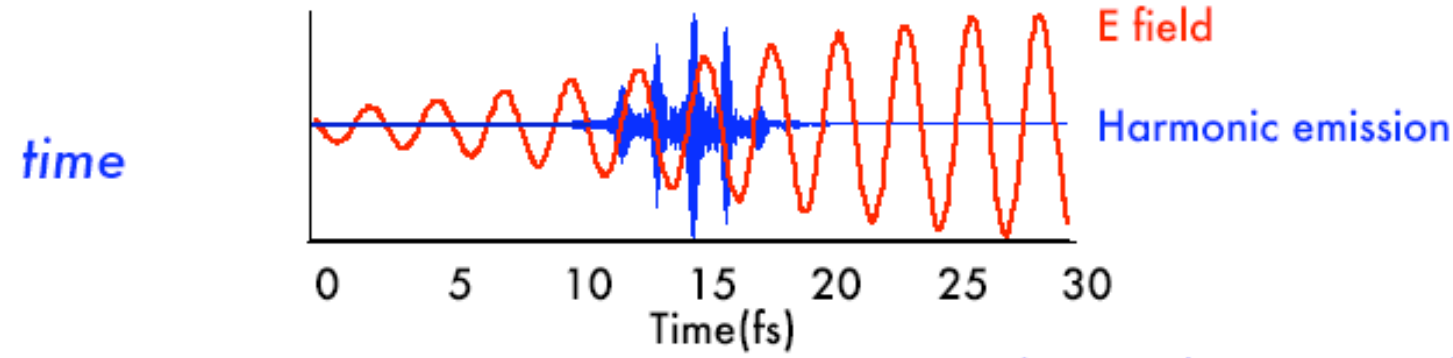

I. Christov et al, PRL 78, 1251, (1997)

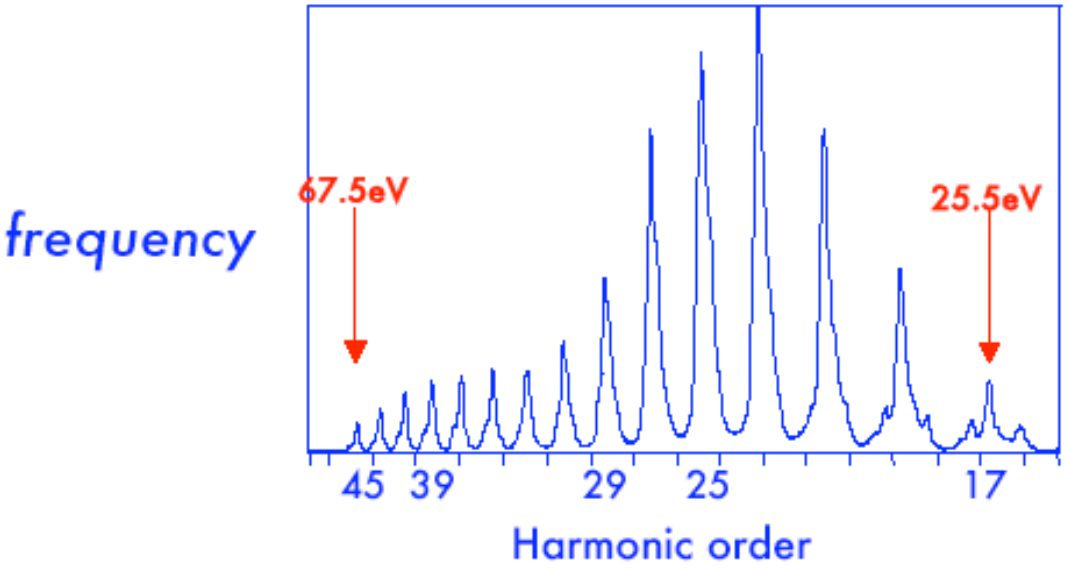

J. Zhou et al, PRL 76(5), 752-755 (1996)

Free electron lasers –FEL 1

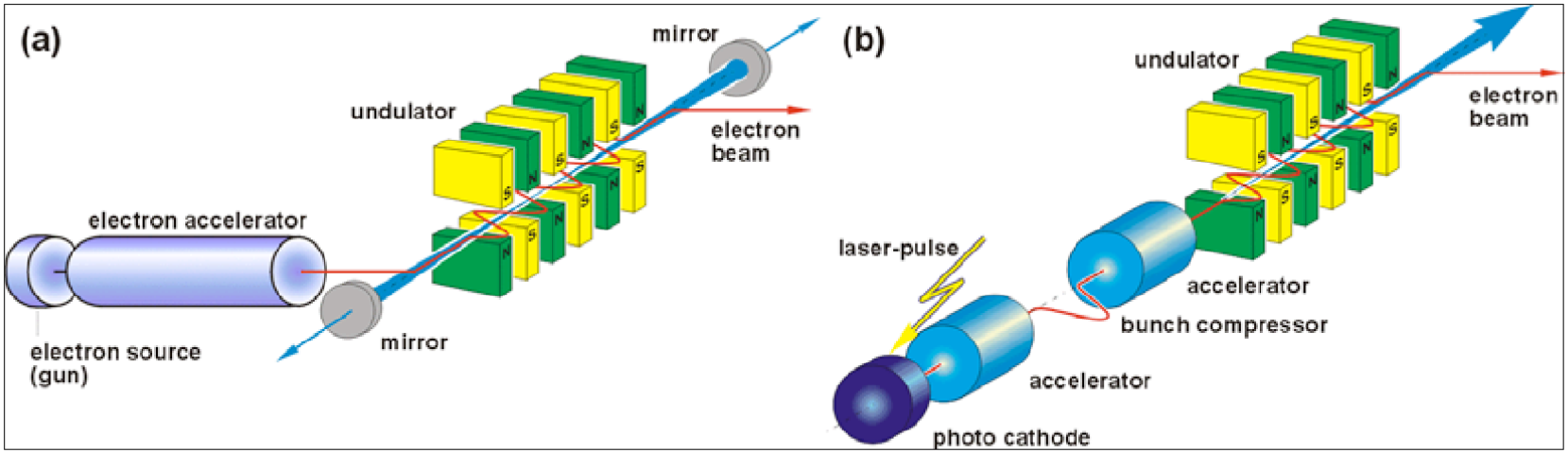

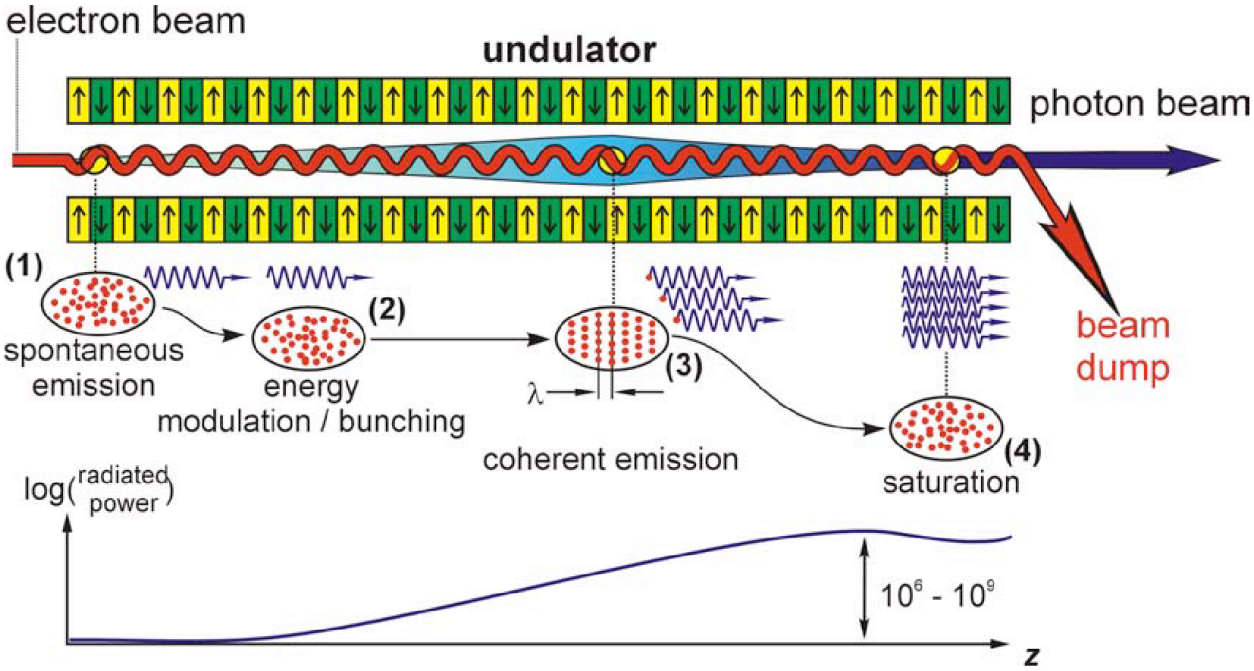

Free electron lasers – FEL 2

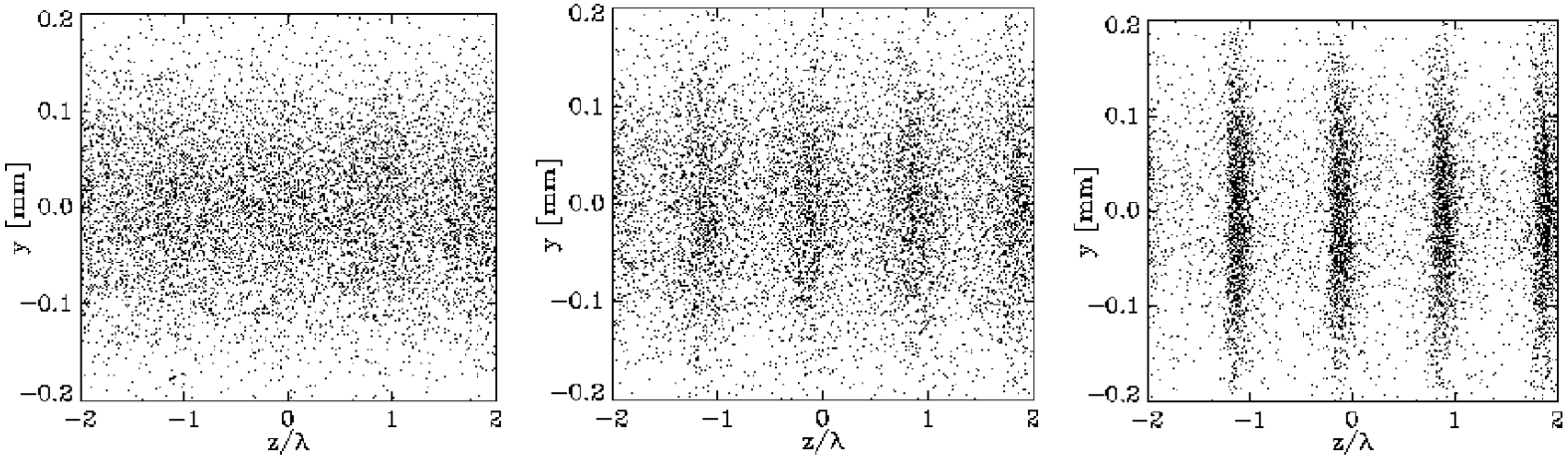

Free electron lasers – FEL 3

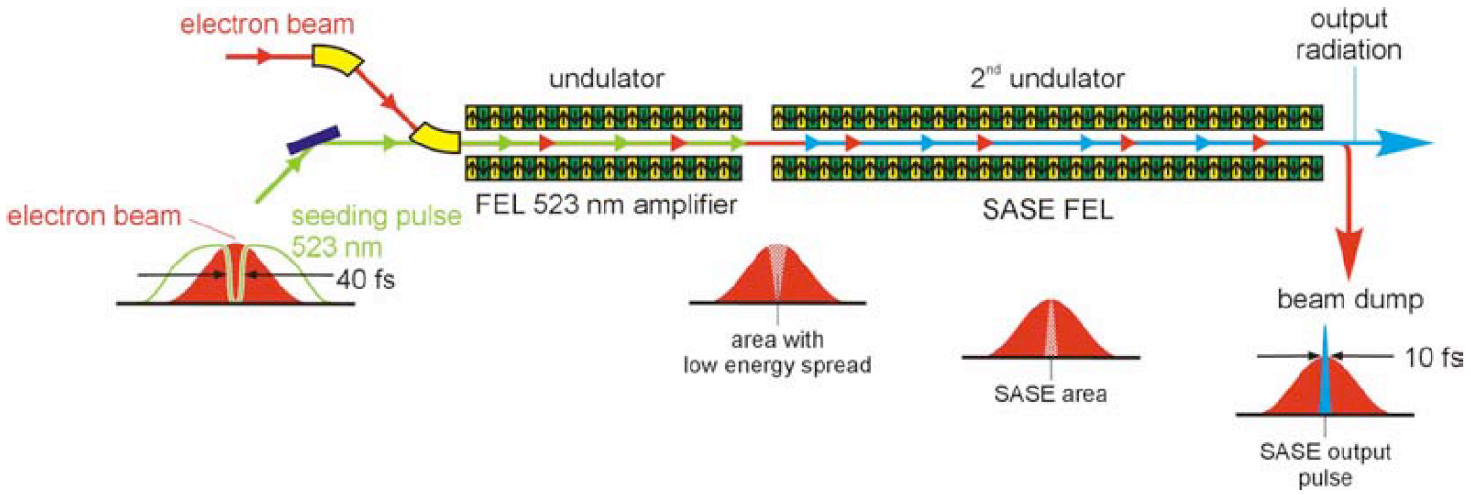

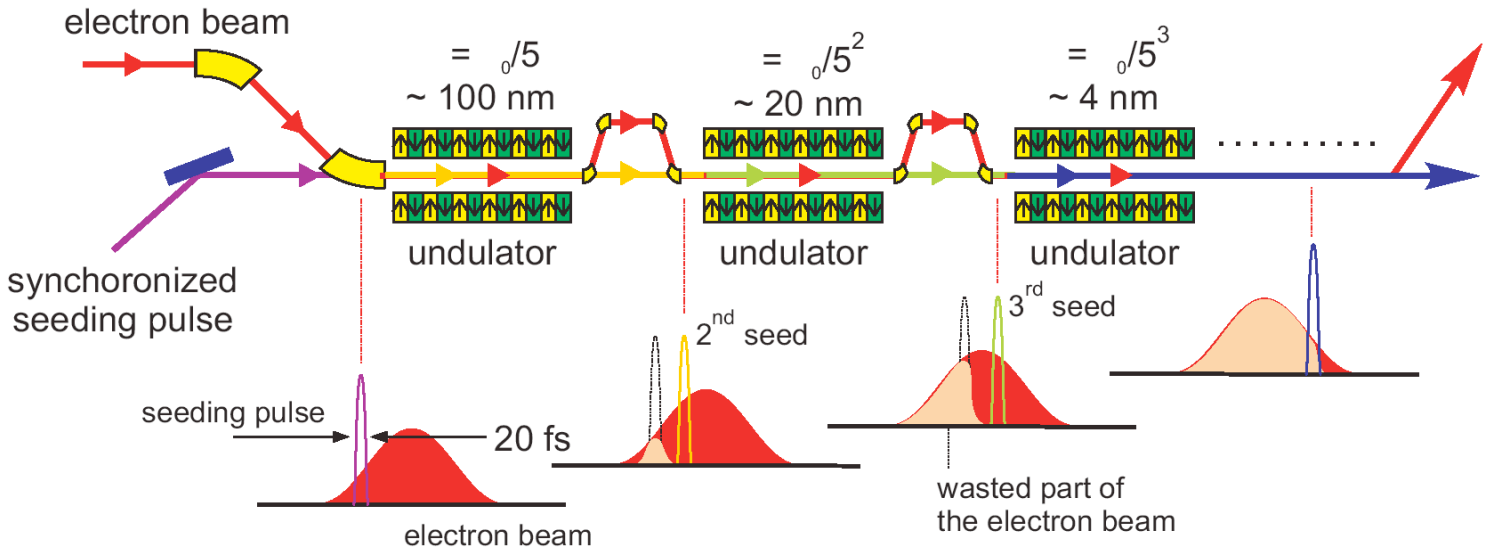

Free electron lasers – FEL 4

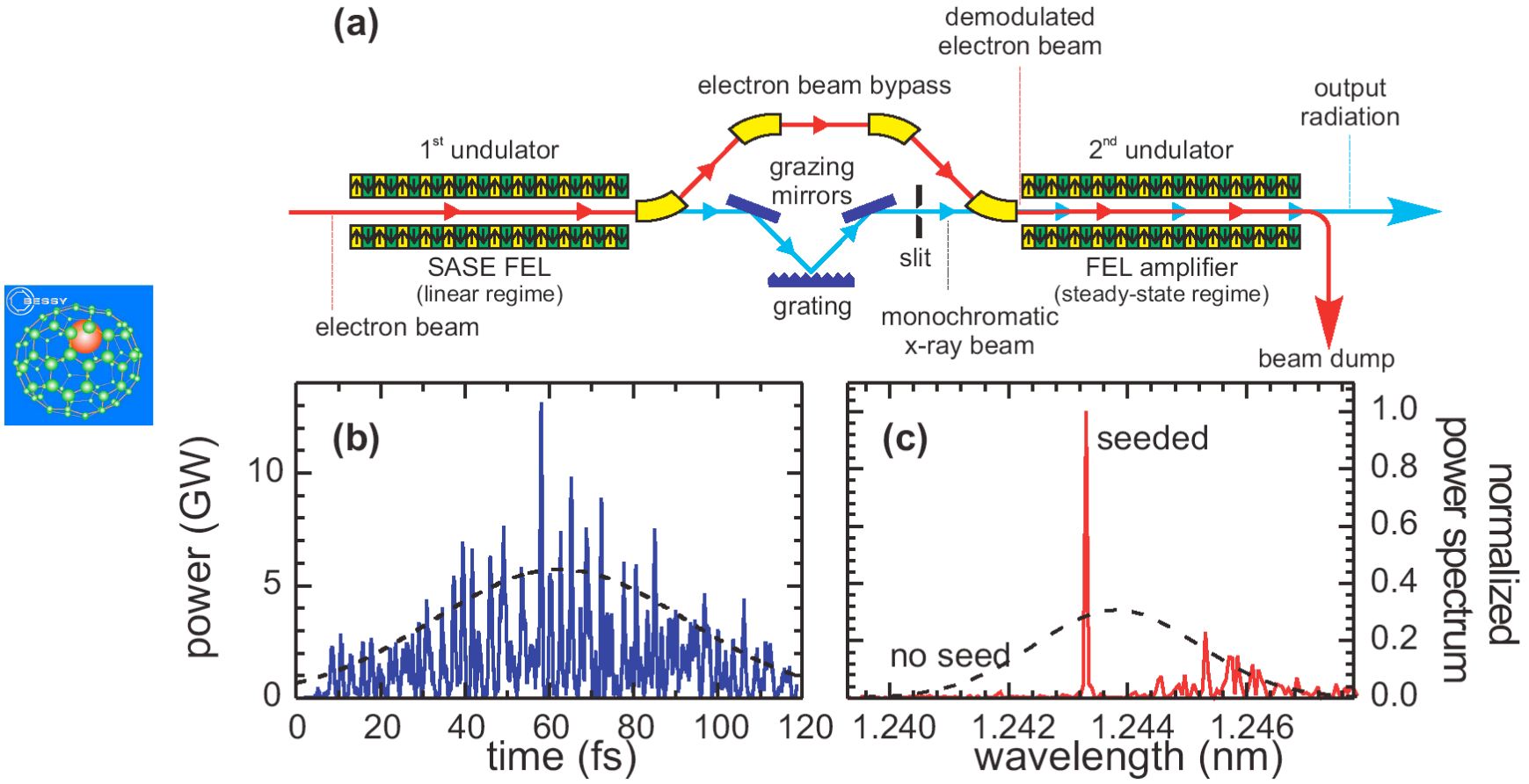

Top: Basic scheme of a two-stage FEL [16] providing full longitudinal and transverse coherent light, see text for details. Bottom: GENESIS simulation of the two-stage FEL employing a 3 kW seed in the second undulator.

FEL Coherence

SASE-FLASH

Courtesy W. Fawley and E. Allaria

PRL 101, 254801 (2008) PHYSICAL REVIEW LETTERS week ending 19 DECEMBER 2008

Transverse-Coherence Properties of the Free-Electron-Laser FLASH at DESY

A. Singer,* I. A. Vartanyants,† M. Kuhlmann, S. Duesterer, R. Treusch, and J. Feldhaus
HASYLAB at DESY, Notkestrasse 85, D-22607 Hamburg, Germany
(Received 21 August 2008; published 18 December 2008)

A general theoretical approach based on the decomposition of statistical fields into a sum of independently propagating transverse modes was used for the analysis of the coherence properties of the new free-electron laser source FLASH operated at 13.7 nm wavelength. The analysis shows that several transverse modes are contributing to the total radiation field of FLASH. The results of theoretical calculations are compared with measurements using Young's double-slit experiment. The coherence lengths in the horizontal and in the vertical directions 20 m downstream from the source are estimated at 300 and 250 μm, respectively.

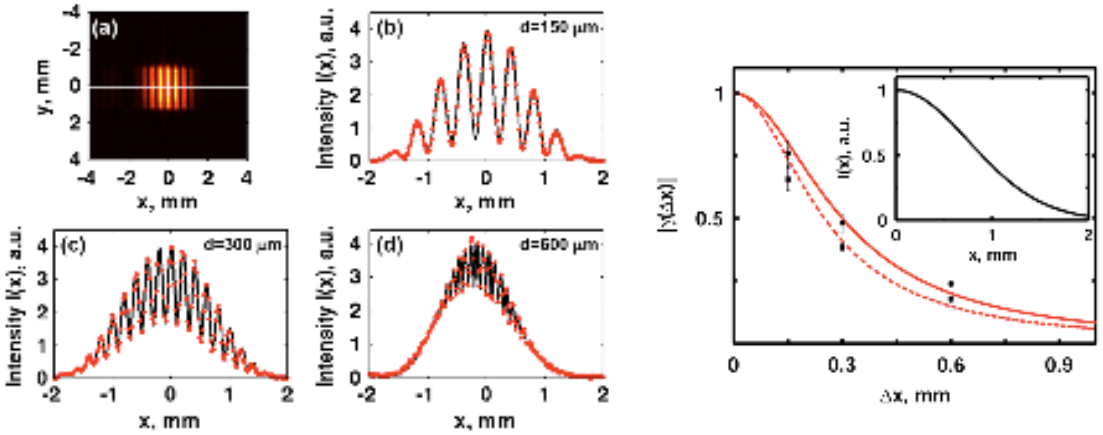

$$\Gamma(\mathbf{r}_1, \mathbf{r}_2, \tau) = \langle E(\mathbf{r}_1, t) E^*(\mathbf{r}_2, t+\tau) \rangle,$$

$$I(P) = I_1(P) + I_2(P) + 2\sqrt{I_1(P) I_2(P)} |\gamma_{12}(\tau)| \times \cos[\omega\tau - \alpha_{12}(\tau)],$$

SASE vs. SEEDED FEL

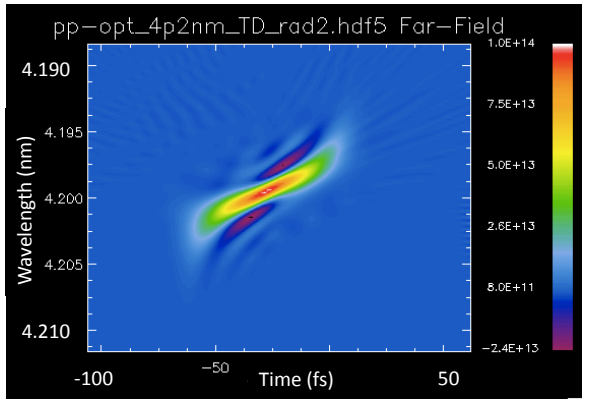

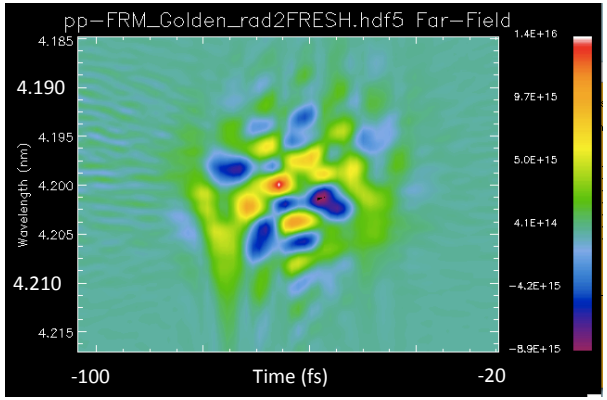

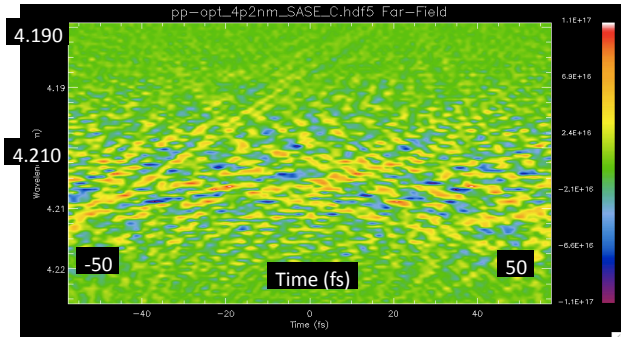

FEL- Science: Nano-materials for energy applications

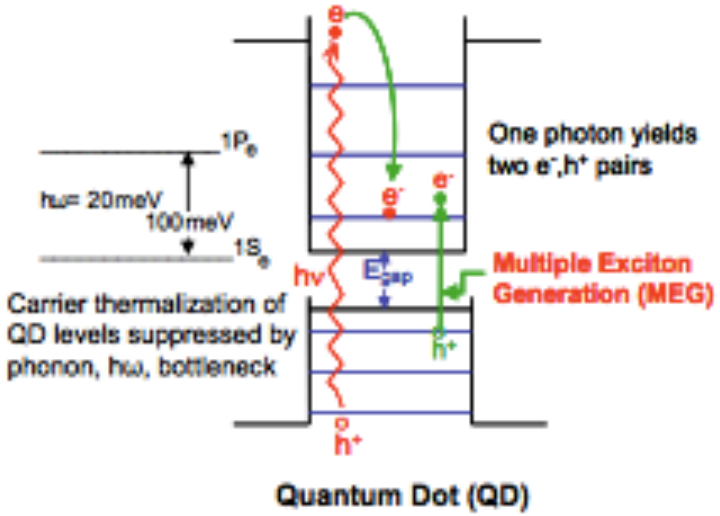

In quantum dots used for solar cell applications, the absorption of one incident photon can lead to the creation of more than one electron-hole pair. This is an inverse-Auger process, which is enhanced in a quantum dot by quantum confinement and the relaxation of the requirement to conserve momentum. Furthermore, thermalization of high-energy carriers is suppressed by the phonon bottleneck produced by the large energy separation of quantized levels. A.J. Nozik, Physica E **14**, 115 (2002).

Because nanoparticle surfaces and interfaces play a key role in multiple exciton generation and its efficiency, it is crucial to understand these interfaces. The small size of the dot makes this a demanding task, requiring much higher average brilliance than today's soft X-ray sources offer. Following **the picosecond relaxation of hot electrons and holes requires 100 femtosecond or shorter X-ray pulses and high peak brightness available** only on next- generation light sources.

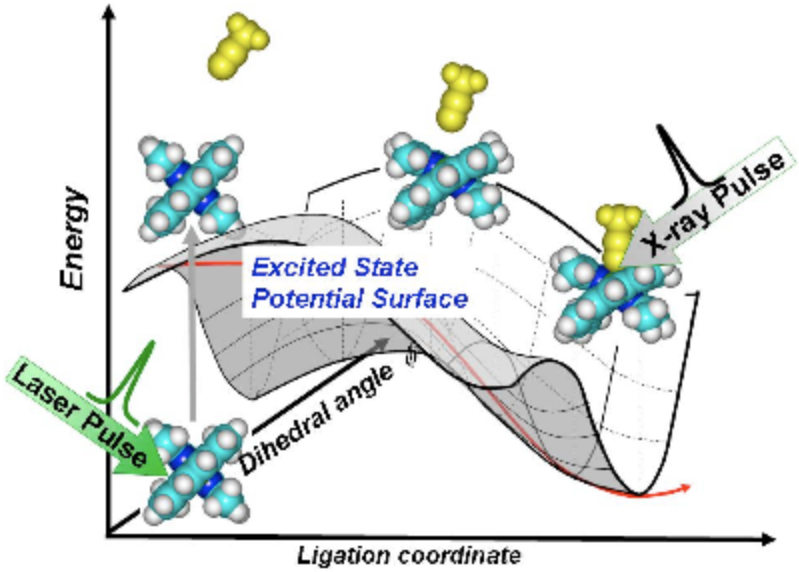

Structural dynamics of a photoactive copper complex excited state created by green laser pulses followed by X-ray pulses to capture both dihedral angle movements on 100-fs time scale and ligation coordinate changes on ps to ns time scale. [Chen et al., J. Am. Chem. Soc. **124**, 10861-10867 (2002); **125**, 7022-7034 (2003); **129**, 2147-2160 (2007)].

FEL- Science: Controlling spin and charge in complex materials

Coherent Manipulation and Time-resolved Imaging of spin and Magnetic Properties

Quantum-dot-based materials are the storage materials with the highest data density known. Coherent rotation of spins in these dots significantly enhances the writing speed of magnetic memory. Using conventional magnetic fields, writing speeds of less than 100 picoseconds can be achieved, whereas with a femtosecond photon pulse, it has been demonstrated that the magnetization can be changed on the 100-femtosecond time scale, although the exact nature of this switching process is not yet resolved.
Time-resolved holographic imaging with circular magnetic X-ray dichroism will allow mapping of the spatially resolved changes in the spin and orbital momentum, following stimulation by a femtosecond laser pulse. This will reveal new details about the transfer of spin momentum to other degrees of freedom, such as the lattice, which enables the change in magnetization. This requires a ***short-pulse, soft X-ray circularly polarized source with a photon energy tuned to individual absorption edges*** and synchronized with an external laser.

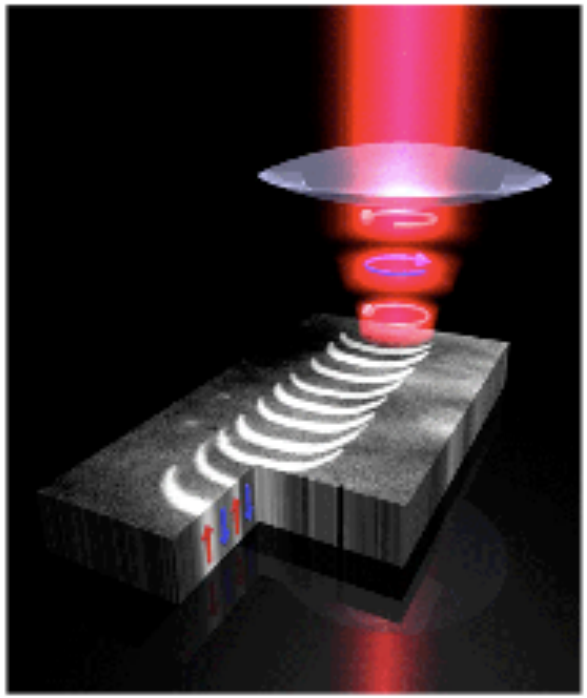

Magnetic domain pattern written by circularly polarized laser pulses. The magnetization reversal is thought to proceed via a coherently excited intermediate state that could be characterized by future light sources. C.D. Stanciu *et al.*, Phys Rev. Lett. **99**, 047601 (2007).

FEL- Science: **Catalysis and the Energy Challenge**

Femtosecond Movies of a Chemical Reaction Capturing and Controlling the Metastable states

Knowledge of the reaction mechanism is central to understanding catalytic reactions. The atomic structure, energies, and electronic structure of the initial reactant state, the final product state, and the activated complex transition state must be characterized for each elementary step. The design of improved catalysts and photocatalysts requires an understanding of how the energetics and dynamics for each step depend on the details of the dynamic structure of the active site and its surroundings, including the reaction media. **Achieving this depth of understanding will require temporal measurements on time scales ranging from 10^{-18} s for electronic excitations, 10^{-15} s for atomic rearrangements,**
to 10^{4} s for macroscopic morphological changes occurring over many reaction cycles. This has to be performed with nanometer spatial resolution, since catalysts are by design inhomogeneous materials
Photoemission microscopy will provide a key approach to this challenge, requiring the highest possible average brilliance of the source in the soft X-ray range.

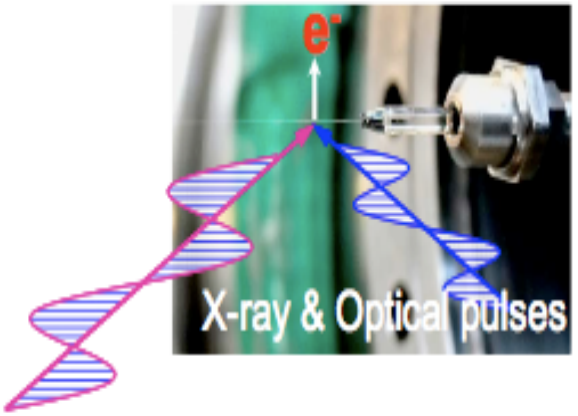

Vacuum liquid micro-jet for photoelectron spectroscopy with femtosecond optical pump and femtosecond X-ray probe pulses (from Bernd Winter (BESSY), 2008).

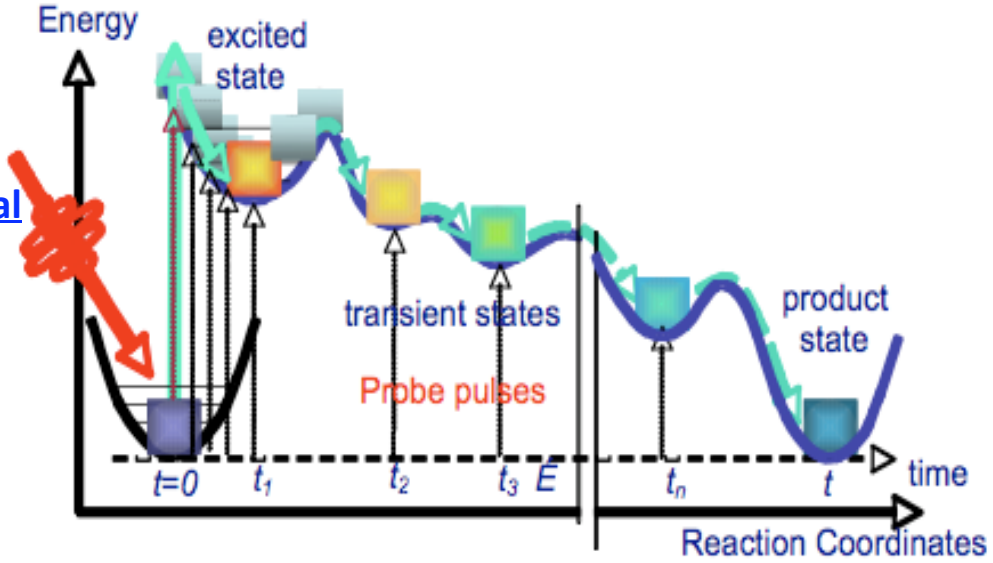

A fs molecular movie. A laser pulse excites the system, and then the resulting cascade of transient states is probed at various time intervals until the product state is formed (image courtesy of Lin Chen, Argonne).

Life Science: Imaging of Cells and Chromosomes

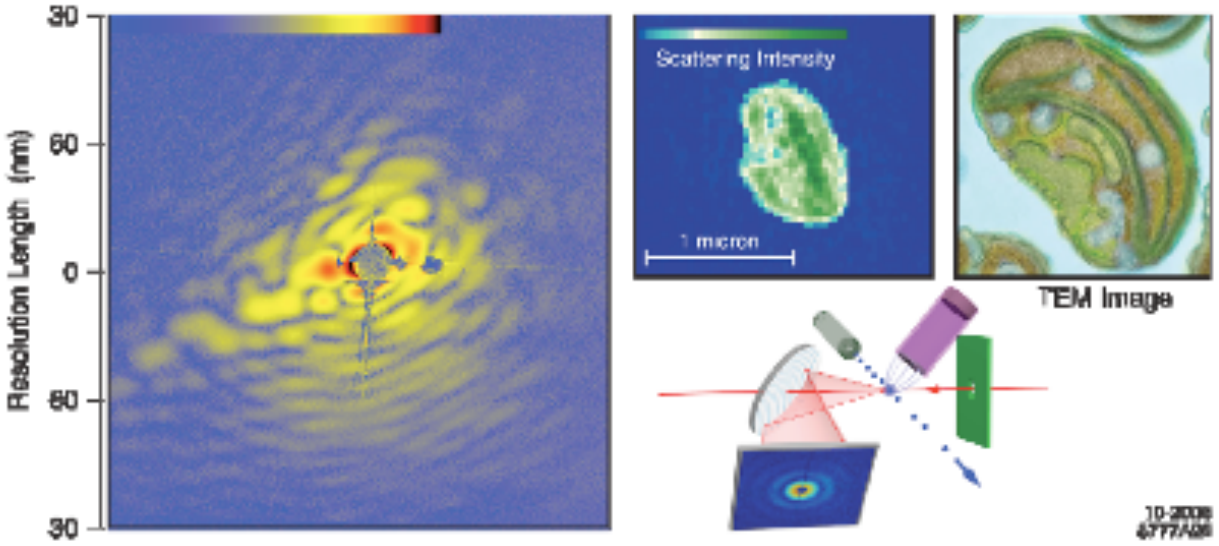

Left: Femtosecond single-shot X-ray scattering pattern. *Top middle:* The reconstructed image of a live picoplankton that was injected at 200 m/s into the beam of the soft X-ray laser FLASH operating at 7-nm wavelength, 15-fs pulse duration, and ~10^{14} W/cm^2 power density; image reconstructed using Shrinkwrap (Sebastien Boutet) (Source: J. Hajdu *et al.*, private communication). *Top right:* transmission electron microscopy (TEM) image (Source: W. Eikrem and J. Throndsen, Univ. of Oslo). *Bottom right:* Schematic setup of the diffraction experiment**. The soft X-ray image can be extended to molecular resolutions with an X-ray laser operating in the wavelength range from 0.5 to 1.5 nm.**

Environmental Science: Imaging Structure and Reactivity Of Individual Nano-particles

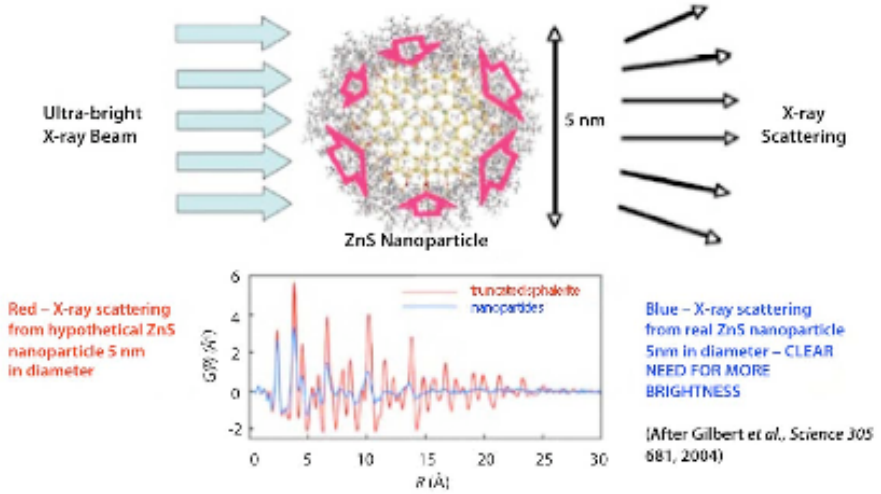

X-ray scattering from a hypothetical individual 5-nm ZnS nanoparticle, compared with experimental scattering from a collection of 5-nm ZnS nanoparticles, **showing the clear need for increased brightness**. B. Gilbert *et al.*, Science **305**, 651 (2004).

FEL- Science: Coherent X-Ray Scattering

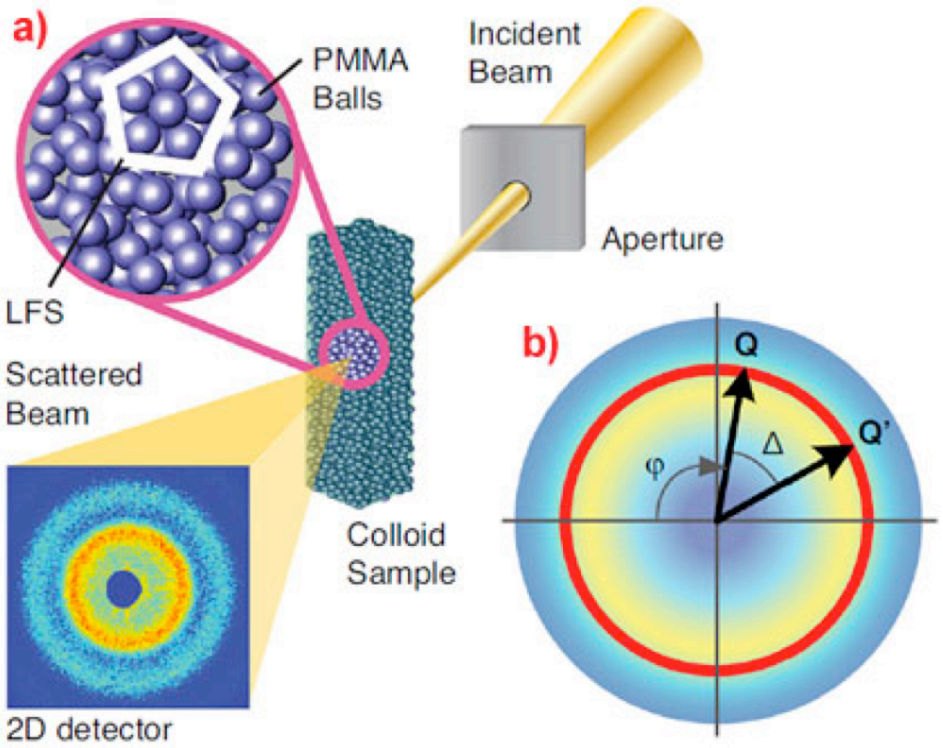

Local symmetries in disordered matter uncovered by coherent X-ray scattering

Local symmetries in colloidal glasses were investigated by **coherent X-ray scattering**. The speckle patterns were analysed by a novel angular cross correlation technique to unravel the hidden local symmetries within the glassy disorder. Four-, 6-, 10- and most prevalently 5-fold symmetries were observed pointing towards locally-favoured structures of icosahedral symmetry.

P. Wochner (a), C. Gutt (b), T. Autenrieth (b), T. Demmer (a), V. Bugaev (a), A.D. Ortiz (a), A. Duri (b), F. Zontone (c), G. Grübel (b), and H. Dosch (a,b),*PNAS* **106**, 11511-11514 (2009)

FEL- Science: Advanced phase contrast imaging

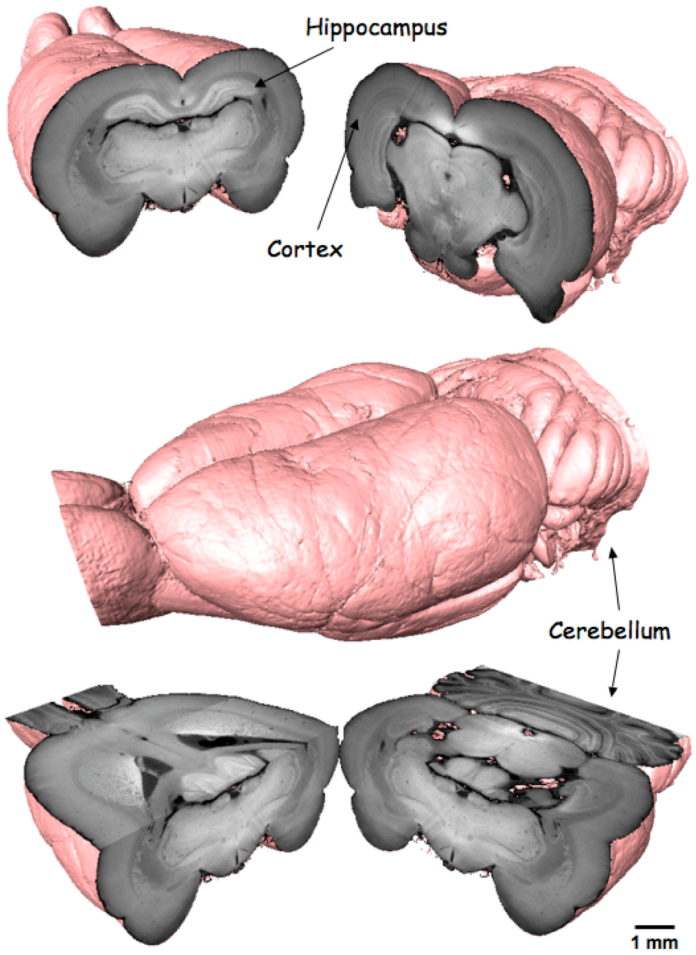

Conventional absorption based X-ray microtomography can become limited for objects showing only very weak attenuation contrast at high energies. However, a wide range of samples studied in biology and materials science can produce significant phase shifts of the X-ray beam and thus **phase contrast X-ray imaging can provide substantially increased contrast sensitivity. A Differential Phase Contrast (DPC) imaging facility, based on grating interferometry,** has been installed at the TOMCAT beamline, with the aim of having a high-throughput of samples in terms of fast data acquisition and post-processing. We have made hardware and software advancements to enable a range of DPC tomographic imaging methods to be applied, such as local and 'widefield' DPC tomography. Darkfield imaging, based on the mechanism of small-angle scattering, provides simultaneous and complementary information about a sample at the micron and the sub-micron length scales. The technique allows the visualisation of the soft tissue features of a rat brain, for example, with a contrast impossible to obtain with conventional absorption-based imaging.

S. A. McDonald, F. Marone, C. Hintermüller, G. Mikuljan, C. David, F. Pfeiffer and M. Stampanoni, J. Synchrotron Rad. 16, 562-572 (2009).

FEL- Science: Properties of individual mass-selected clusters

Direct structural determination and manipulation of individual size-selected clusters constitute major scientific grand challenges in nanoscience. The physical and chemical properties of atomic clusters change dramatically with size and structure, a fundamental feature of nanoscience. Size-selected clusters provide the best-defined models for heterogeneous catalysts.

Furthermore, size-selected clusters provide the means to discover and fabricate tailor-made new materials with specific magnetic, optical, or electronic properties. Atomic structures are the most fundamental properties of size-selected clusters, but there are currently no experimental methods for directly determining them.

Multiple complementary techniques must be exploited for the characterization of these dilute systems. These include **XPS for chemical characterization and structural information, ultraviolet photoelectron spectroscopy for electronic properties, circular magnetic X-ray dichroism for magnetic properties, and EXAFS** for structural determination. Still, the number of clusters in the trap, 10^4 to 10^6, is too small to allow reliable EXAFS measurements. Good signal-to-noise data should be obtainable, given the high average brilliance of ***the next-generation sources supplying 10^{16} to 10^{18} photons per second and their tunability.*** The most exciting prospect would be to use a single intense X-ray pulse to scatter off a single size-selected cluster to yield its entire three-dimensional structure.

Such experiments may be within reach with the high peak brilliance of next-generation light sources and the development of sophisticated scattering analysis procedures.

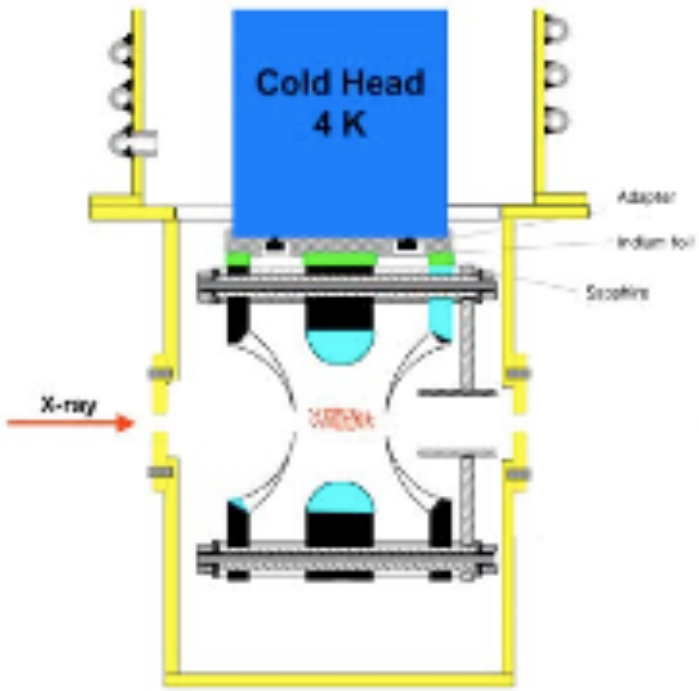

A temperature-controlled ion trap for EXAFS of size-selected clusters. X.B. Wang and L.S. Wang, Rev. Sci. Instrum. **79**, 073108 (2008).

Magnetic Dynamics

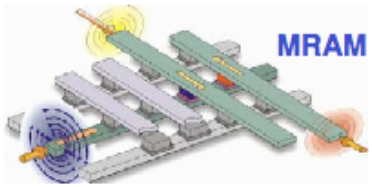

imaging ns - ps magnetization dynamics

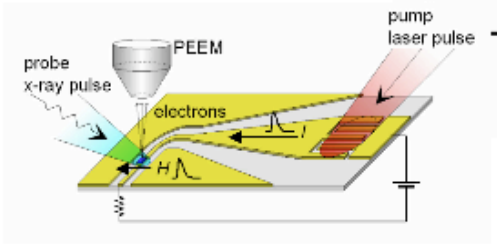

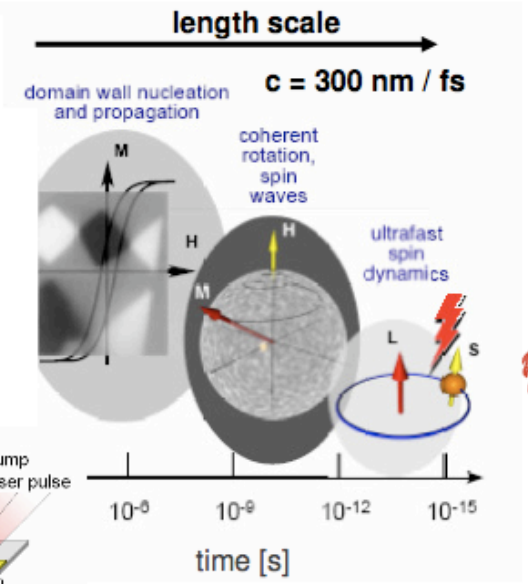

fs electron-spin dynamics

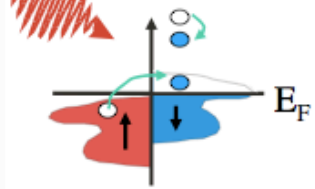

H. Duerr (SLAC)

coherent excitation of magnons

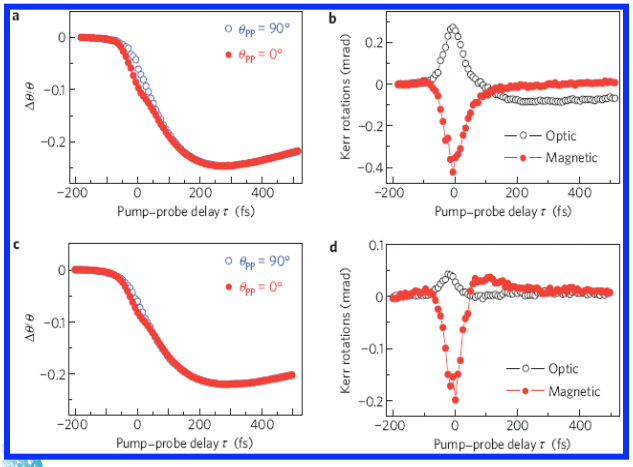

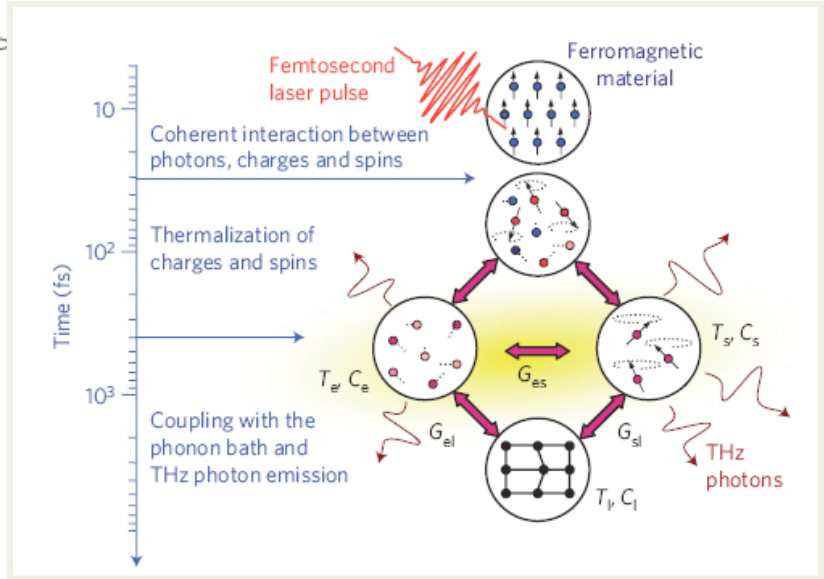

FEL- Science: Magnetic Scattering for Vortex in SC

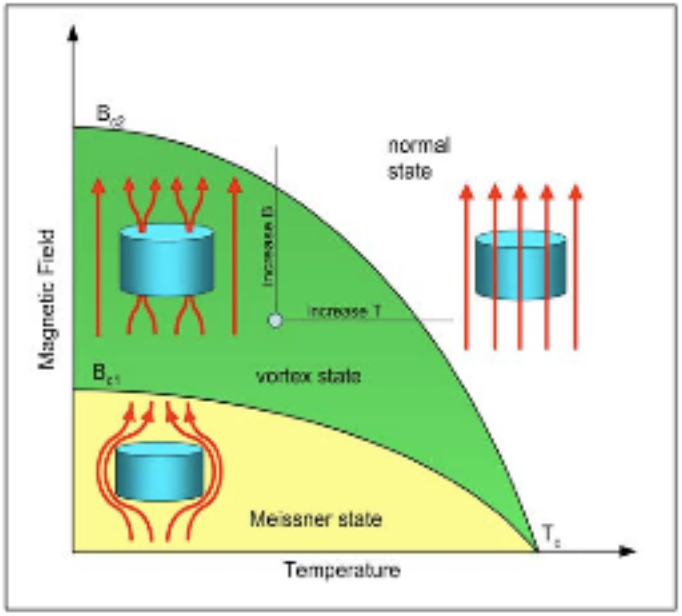

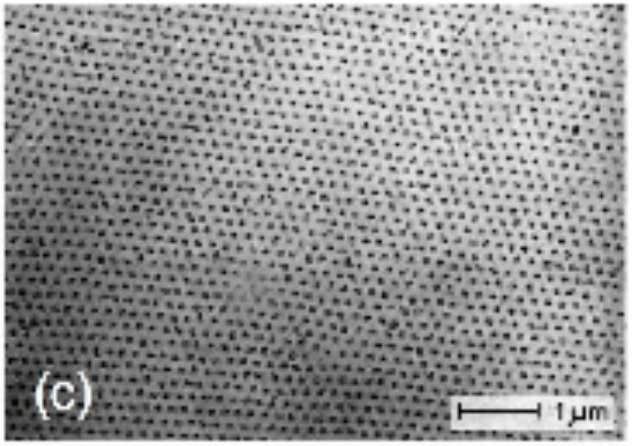

U. Essmann, unpublished; see also *Phys. Lett*. ***24A, 526 [1967])***

C. Giannetti, IEEE Photonics Journal (2009)

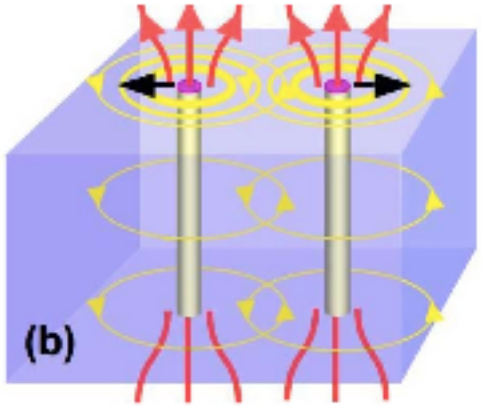

DOE REPORT on SC, 2006

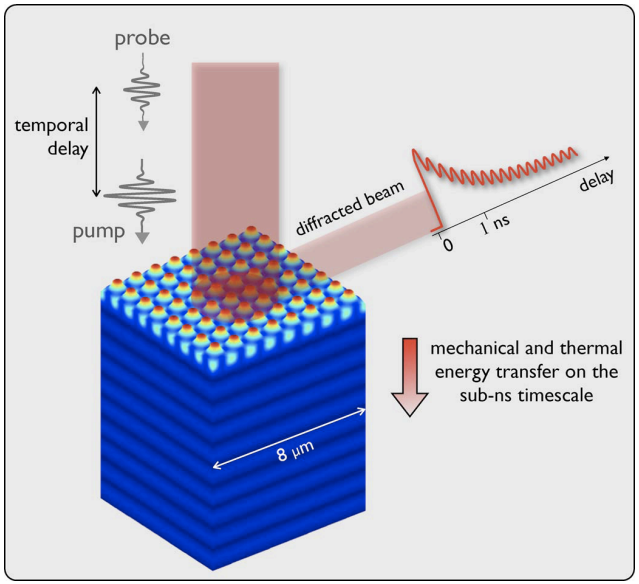

FEL- Science: Low Density Matter

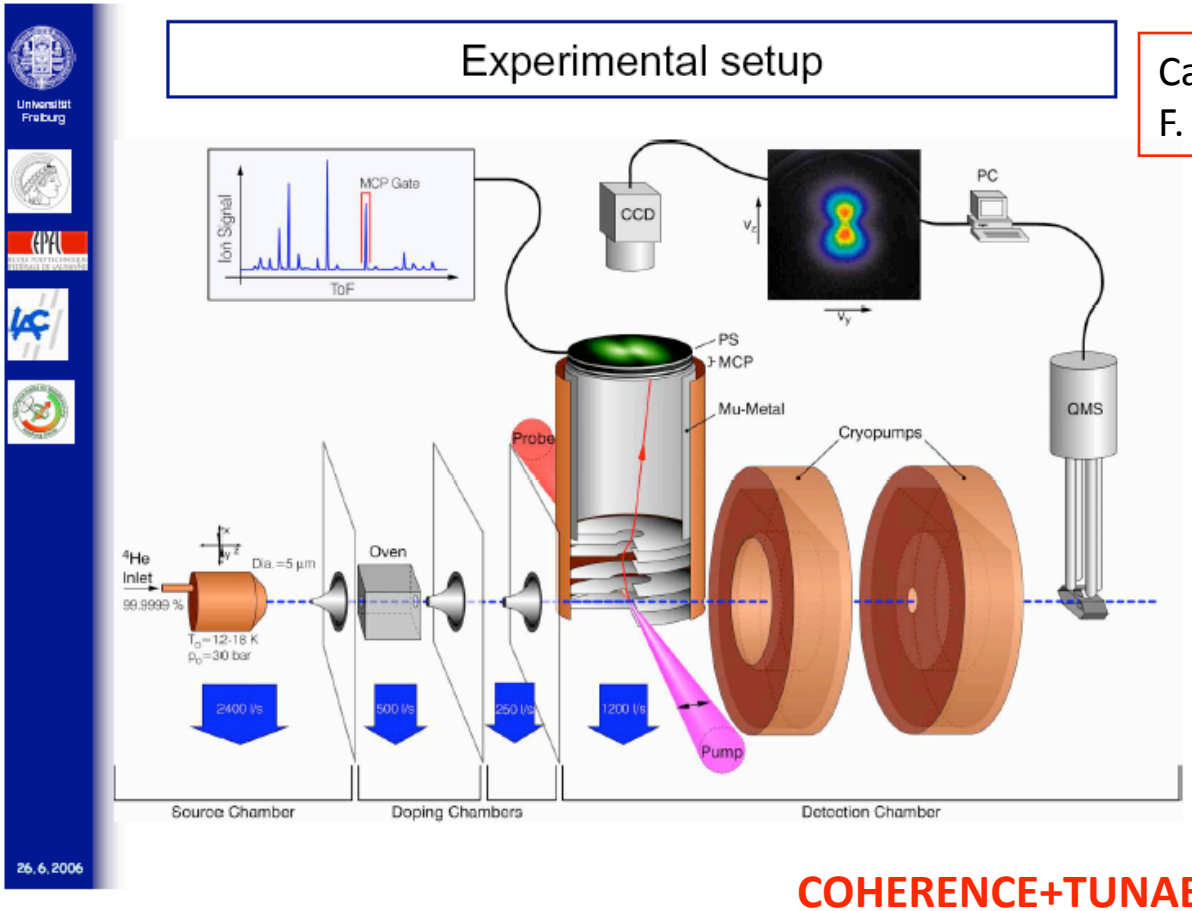

Carlo Callegari: LDM coordinator
F. Stienkemeir: End station spoke person

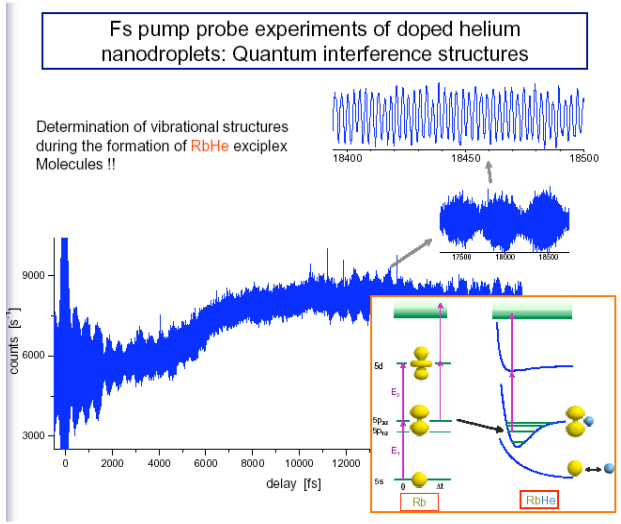

COHERENCE+TUNABILITY+POLARIZATION

Cluster and nanoparticle spectroscopy

Spokespersons: **F. Stienkemeier,** (Univ. of Freiburg-D); **T. Moeller** (Frei University, Berlin)

Co-proponents :K.Fauth (MPI- Stuttgart, D), M. Drabbels (EPFL- CH), M. Schmidt(CNRS –Orsay, Fr), U.Buck (MPI-Goettingen, D)

FEL- Science: The 10^{-18} s Challenge with 0.1-1 keV soft X-ray

Attosecond science

Nature Physics, June 2007

The motion of electrons on the atomic scale has been hidden from direct experimental access until recently. We review the revolution in technology that opened the door to real-time observation and time-domain control of atomic-scale electron dynamics, and address the expected implications of having the tools to monitor electrons with sub-atomic resolution in both space and time.

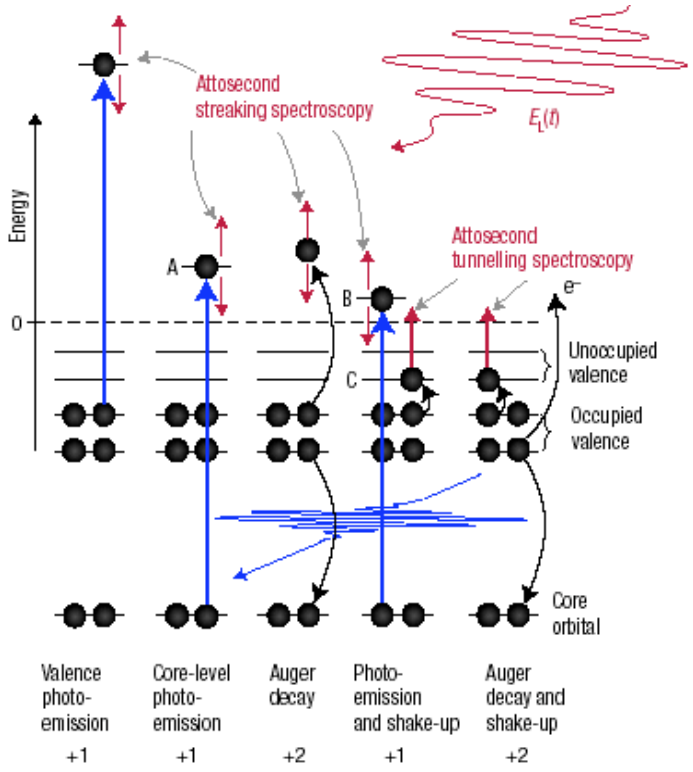

Excitation and relaxation. Electronic excitation and relaxation processes in atoms, molecules and solids, and possible ways of tracing these dynamics in real time. The labels 1+ and 2+ indicate single and double ionization.

Attosecond Spectroscopy

REVIEW

The Future of Attosecond Spectroscopy

Philip H. Bucksbaum

Attoscience is the study of physical processes that occur in less than a fraction of a cycle of visible light, in times less than a quadrillionth of a second. The motion of electrons inside atoms and molecules that are undergoing photoionization or chemical change falls within this time scale, as does the plasma motion that causes the reflectivity of metals. The techniques to study motion on this scale are based on careful control of strong-field laser-atom interactions. These techniques and new research opportunities in attosecond spectroscopy are reviewed.

10 AUGUST 2007 VOL 317 SCIENCE

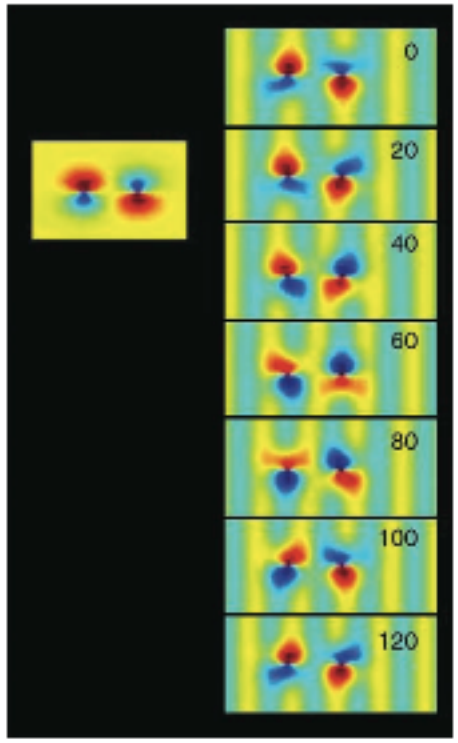

Fig. 2. (Left) Wave function simulating the most weakly bound electron in carbon dioxide, consisting of two p_π orbitals separated by 2.32 Å. Red and blue parts of the wave function are π radians apart in quantum phase. (Right) Coherent scattering of a 25-eV electron from the carbon dioxide orbital out of which it was recently ejected by a strong laser field. The returning electron is incident from the right, and several views are shown over a 120-as time interval. The relative time (in attoseconds) is shown in the top right of the frames. Motion of the wave function is due to interference with the incoming electron.

A few new directions in photoemission measurements

Curtesy C. Fadley, UC Davis & ALS

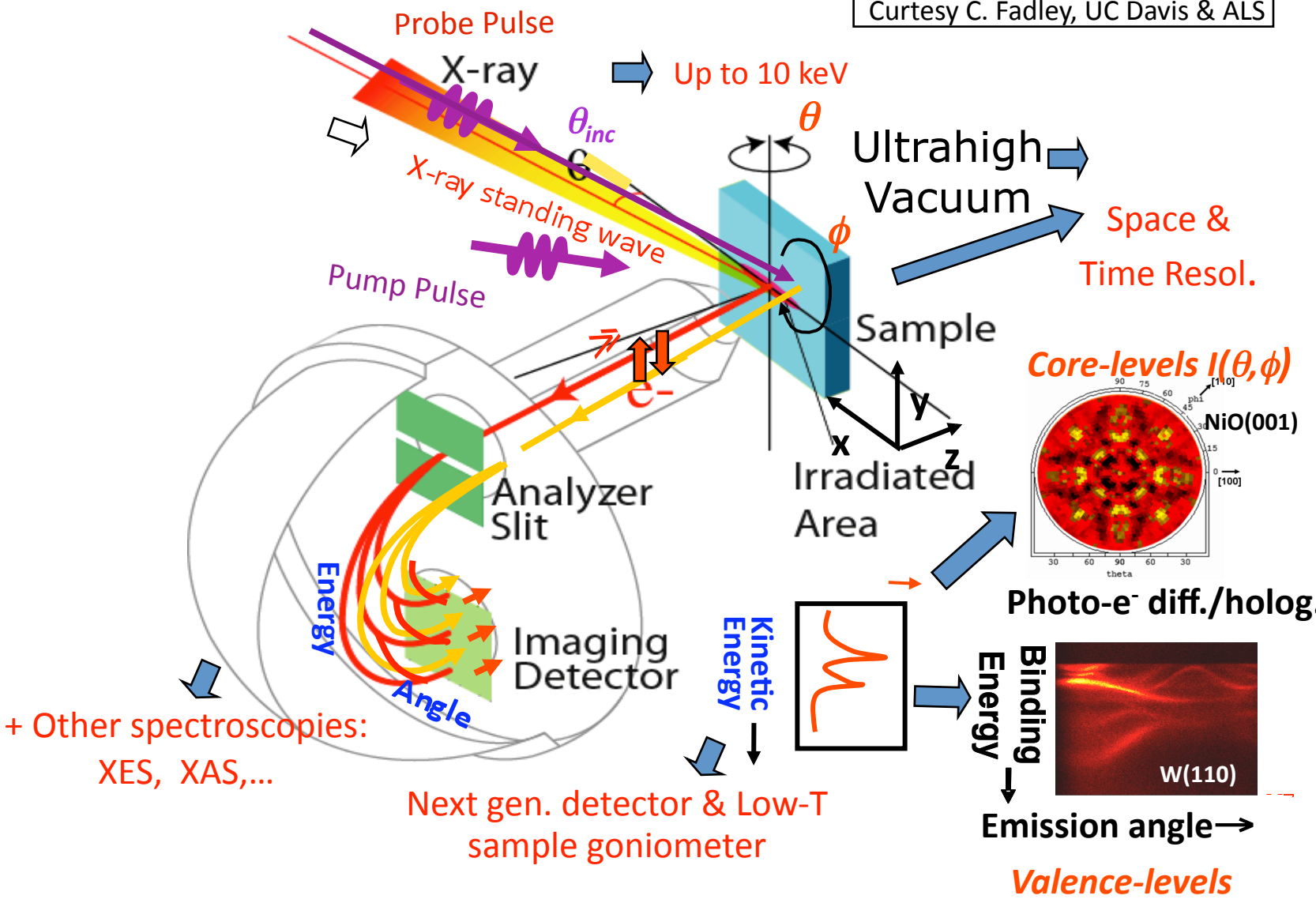

FEL- Science: Space charge in photoemission

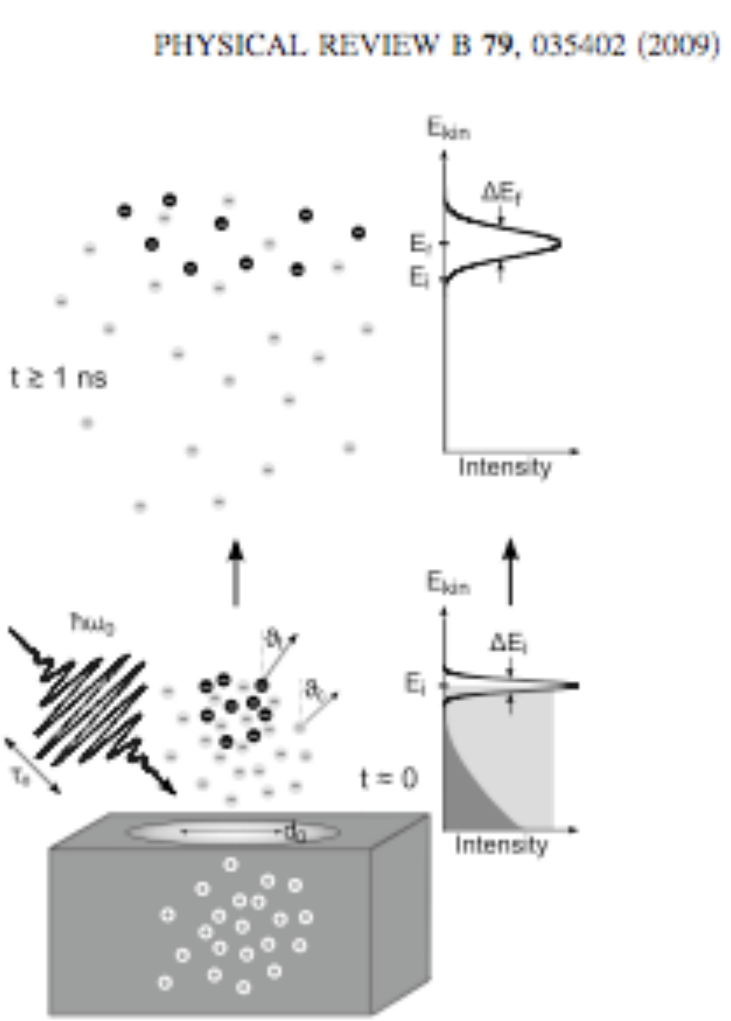

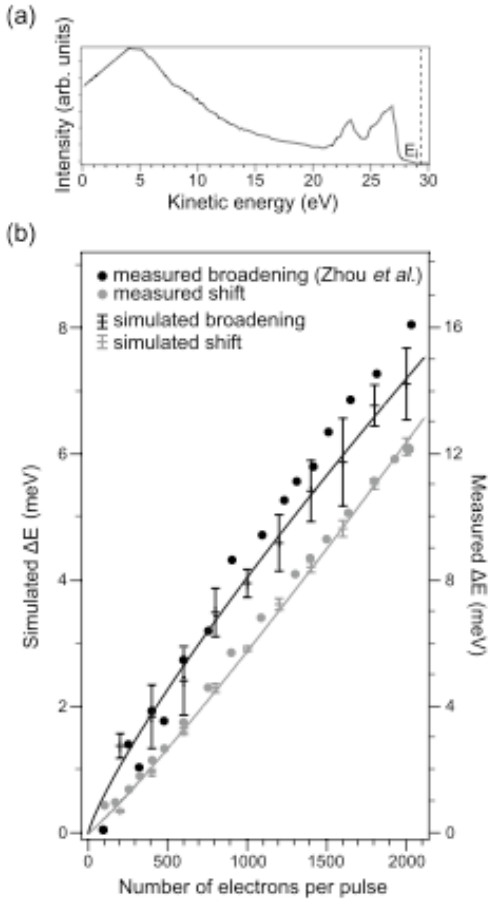

FIG. 3. Space-charge effects on the photoemission spectrum of a polycrystalline gold sample under irradiation with τ_0 =60 ps, $\hbar\omega_0$=34 eV photon pulses. (a) Typical energy distribution curve with the Fermi cutoff at 29.38 eV (taken from Ref. 9). (b) Comparison between simulated and measured (Ref. 9) Fermi edge shifts and broadenings in the range of (0–2000)e^- per pulse. Note the different scales of the vertical axes. Power-law fits to the simulated energy shift and broadening serve as guides for the eyes ($\Delta E_{shift} \propto N_e^{1.11}$, $\Delta E_{broad} \propto N_e^{0.83}$). The spot size is 0.43×0.3 mm^2 and the test electrons are emitted with an angle of 45°. In the simulation, a cosine distribution of the cloud electron emission angles is used.

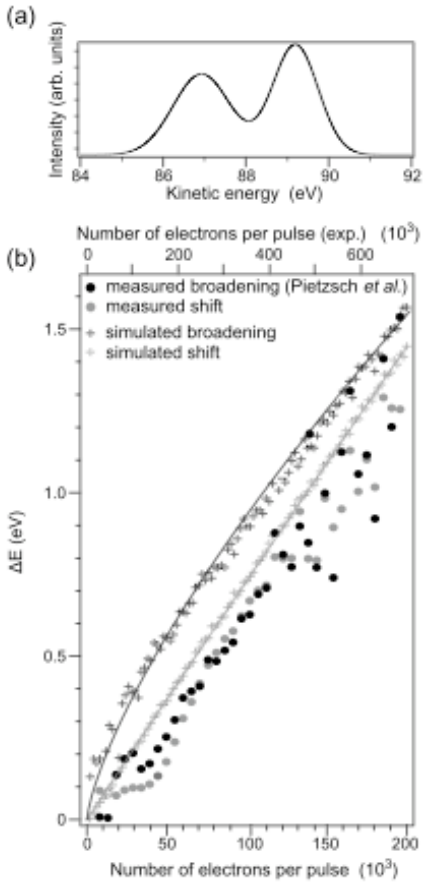

FIG. 5. Space-charge effects on a W 4f core-level spectrum under irradiation with τ_0=40 fs, $\hbar\omega_0$=118.5 eV photon pulses. (a) Typical energy distribution curve with photoemission peaks at kinetic energies of ~87 and ~89 eV (taken from Ref. 21). (b) Comparison between simulated and measured (Ref. 21) peak shifts and broadenings in the range of (0–200 000)e^- per pulse. Note the different scales of the axes for the simulated (bottom axis) and measured data (top axis). Power-law fits to the simulated energy shift and broadening serve as guides for the eyes ($\Delta E_{shift} \propto N_e^{0.98}$, $\Delta E_{broad} \propto N_e^{0.77}$). The spot size is 0.27×0.4 mm^2. In the simulation, a cosine distribution of the cloud electron emission angles is used and the test electron acceptance angle is set to 13°.

FEL- Science: slelective excitations

Selective excitations (CT and phonons) to study transient states and photo-induced phase transitions.
Superconductors (e-ph interactions, magnetism and superconductivity).
Magnetic materials (dynamics of the magnetic excitations).
Strong correlations in hard- and soft- condensed matter (charge transfer and phonon assisted excitations).

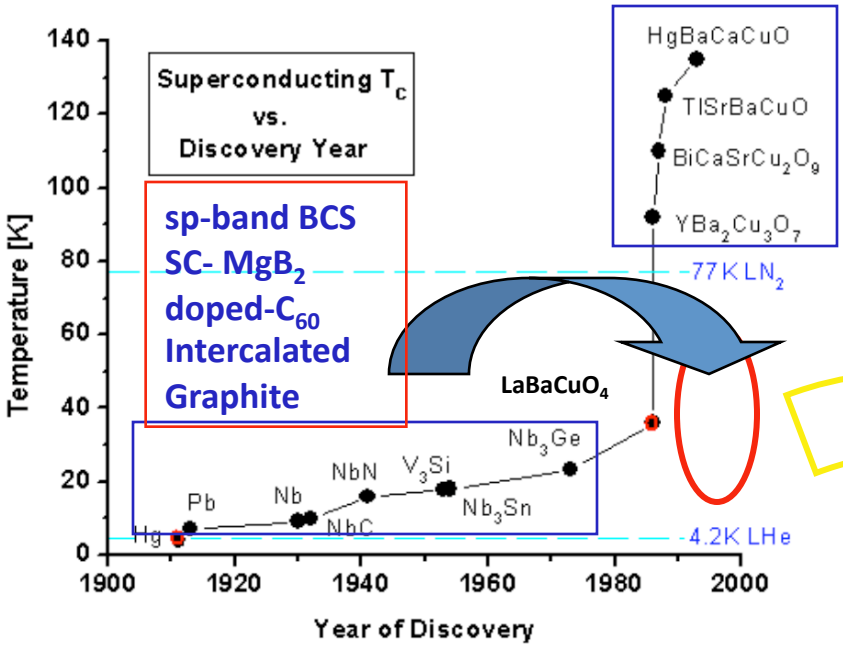

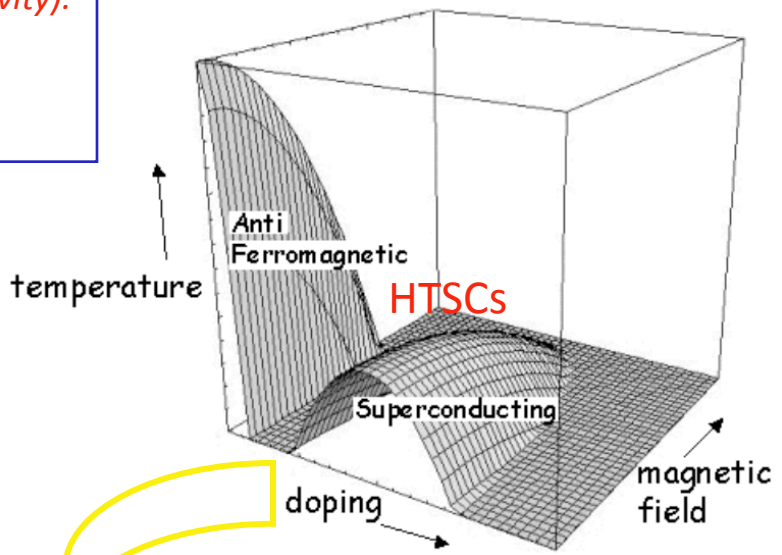

e-ph

?

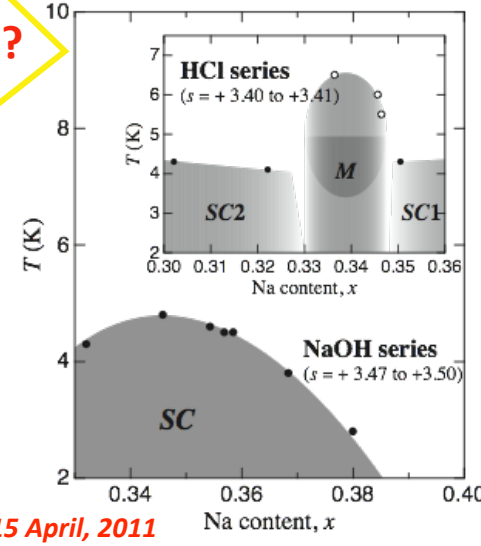

$$\lambda_{\nu\mathbf{q}} \equiv \frac{1}{\pi N(0)} \frac{\gamma_{\nu\mathbf{q}}}{\omega_{\nu\mathbf{q}}^2}. \qquad N_n(0) \equiv \sum_{\mathbf{k}} \delta(\varepsilon_{n\mathbf{k}})$$

$$\frac{\gamma_{\nu\mathbf{q}}}{\omega_{\nu\mathbf{q}}} = 2\pi \sum_{nm\mathbf{k}} |g_{\nu,n\mathbf{k},m(\mathbf{k}+\mathbf{q})}|^2 \delta(\varepsilon_{n\mathbf{k}}) \delta(\varepsilon_{m\mathbf{k}+\mathbf{q}}).$$

$$g_{\nu,n\mathbf{k},m(\mathbf{k}+\mathbf{q})} = \langle n\mathbf{k} | \delta V(\mathbf{r}) | m(\mathbf{k}+\mathbf{q}) \rangle / \delta Q_{\nu\mathbf{q}}$$

FEL- Science: Spin resolved dynamics

Time-of-Flight analyser
@ high operating frequency
(up to 5 MHz)

Spin states dynamics

Objective

The goal of this project is to measure the spin resolved band dispersion and spin dynamics in solid by harmonics and high harmonics generated from a 250 kHz Ti:SA amplified source

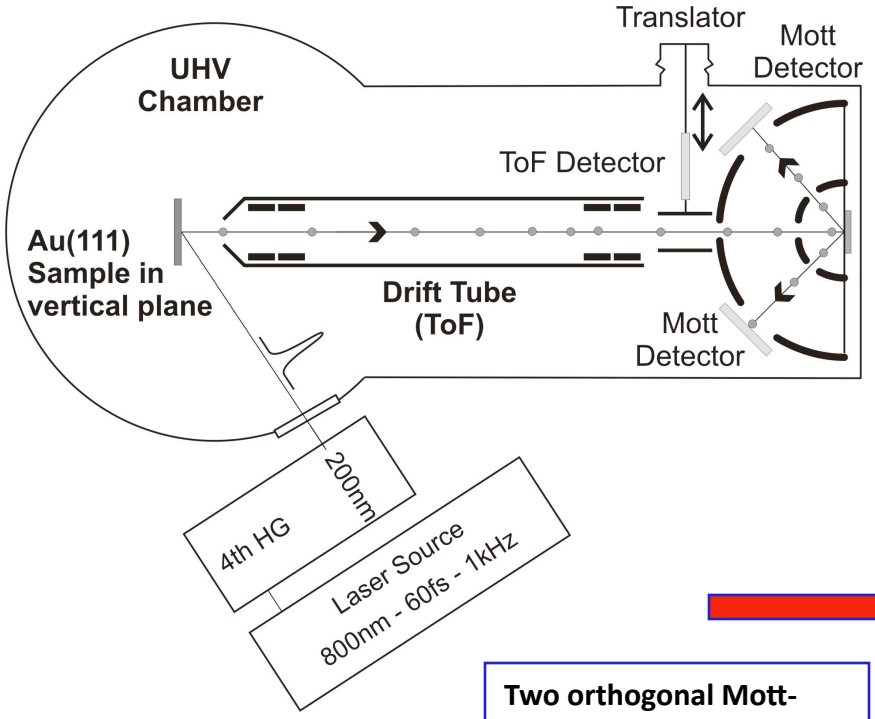

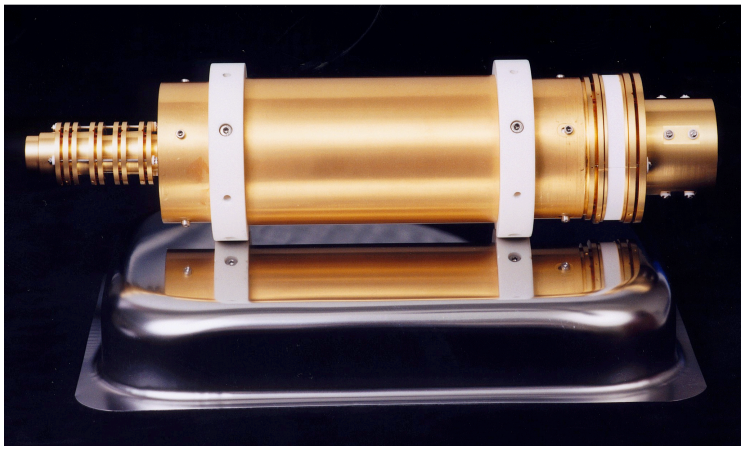

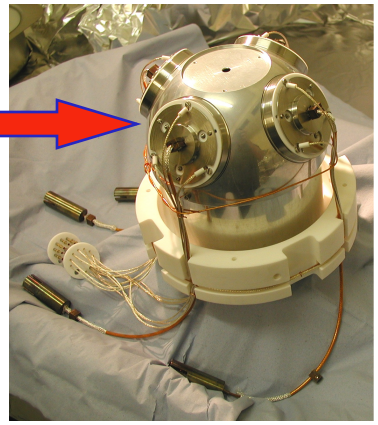

Two orthogonal Mott-detectors to measure V and H spin components

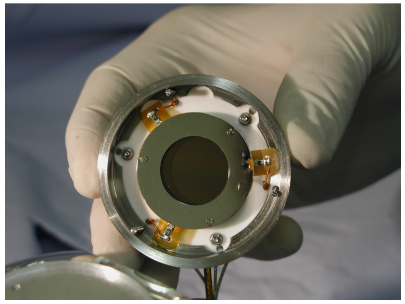

Collaboration with 4GLS (E. Seddon and C. Cacho)

Electron detector

Mott polarimeter

Test of the SR-TR ToF on the Au(111) surface states

- ✓TR- and AR-Photoemission
- ✓Time and Spin resolved experiments
- ✓Fermi surface mapping

Spin-orbit coupling $H_{SO} = \frac{1}{2c^2}\vec{S}\cdot(\vec{\nabla}V \times \vec{p})$

$$V(\vec{r}) = V_0(r,z) + V_3(r,z)\sin 3\varphi + V_6(r,z)\cos 6\varphi$$

$$\vec{\nabla}V = \alpha\,\vec{z} + \beta\,\vec{u}_\varphi \qquad \vec{p} = p\,\vec{u}_r$$

$$H_{SO} = \frac{p}{2c^2}(\alpha\vec{S}\cdot\vec{u}_\varphi + \beta\cos 3\varphi\,\vec{S}\cdot\vec{u}_z)$$

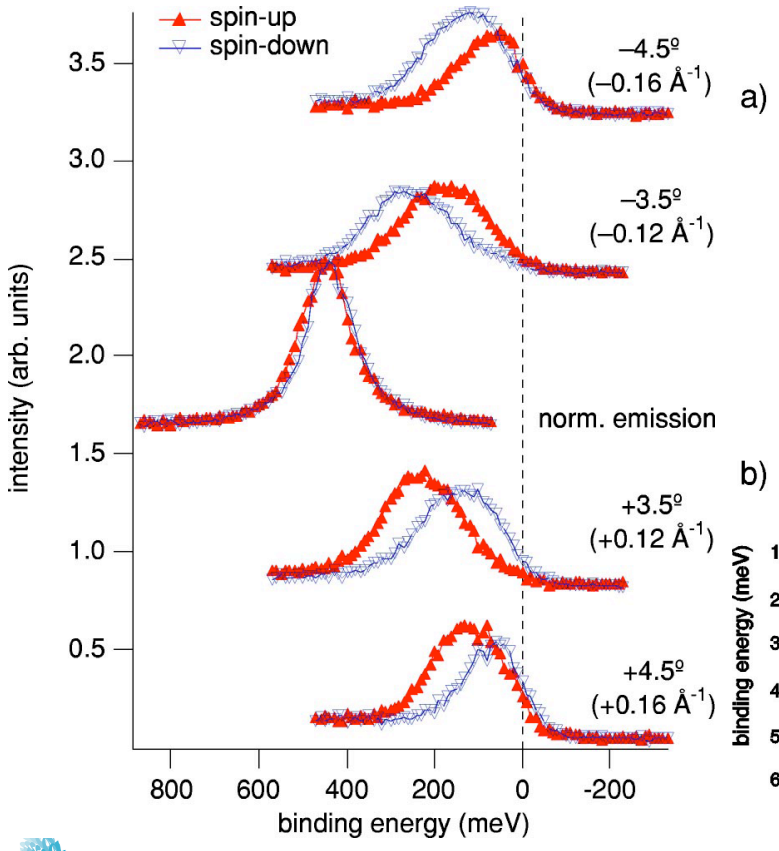

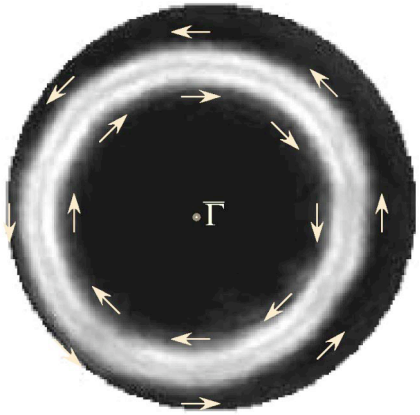

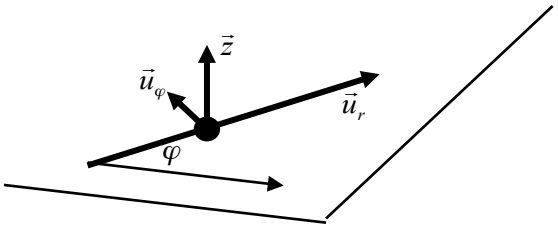

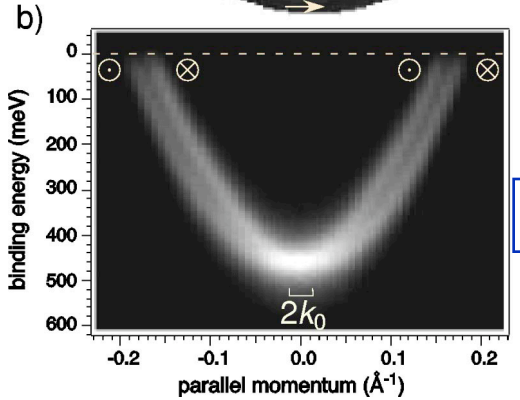

Osterwalder et al. PRB 69 pp.241401R, 2004)

FEL- Science: Spin resolved dynamics

High resolution of the SS energy position

Spin integrated Intensity

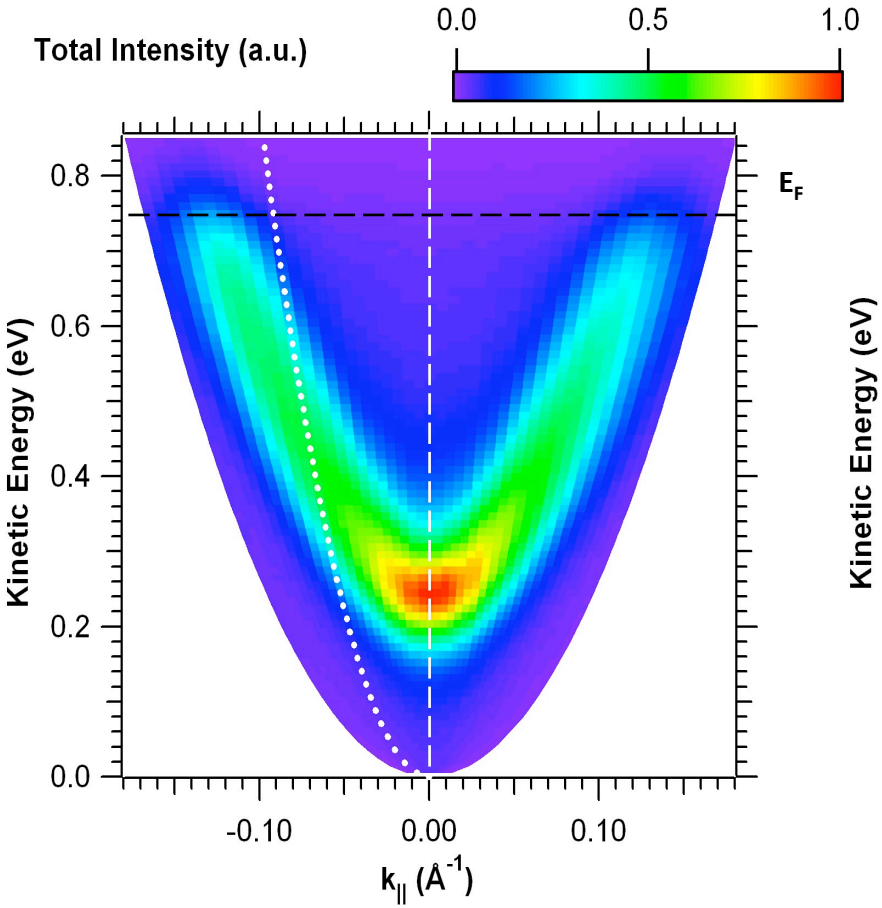

Energy position of the surface states.

Determination of the SS kinetic energy position with very high precision (±2meV).

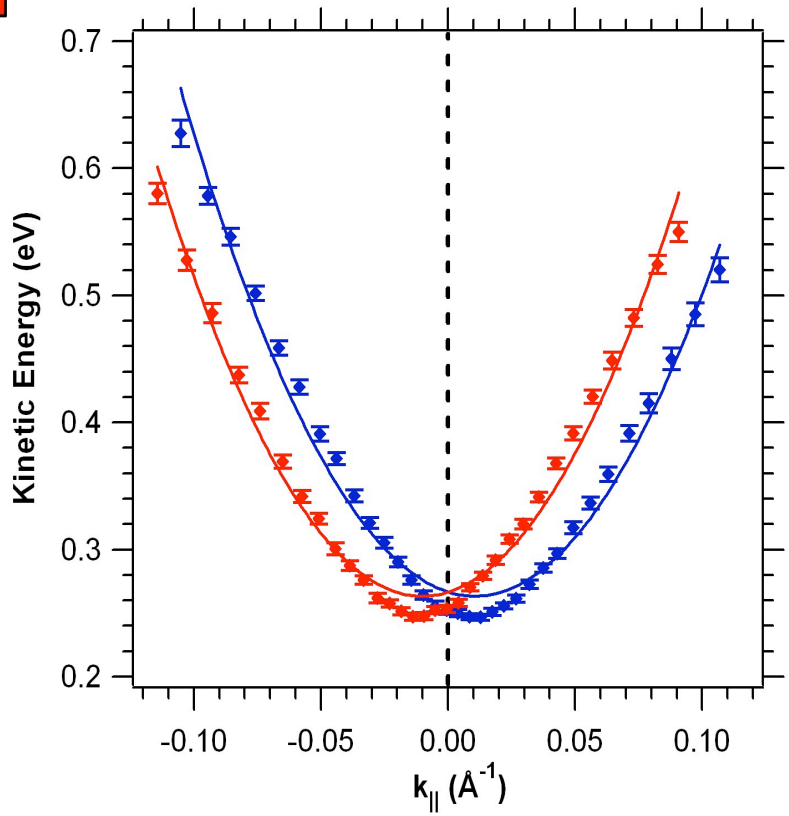

$$E_{\pm} = E_0 + \frac{\hbar^2}{2m^*} \cdot \left(k_{\parallel} \pm k_0 \right)^2$$

E_0 = 260 meV
m* = 0.134
k_0 = 0.011 Å^{-1}

Radiation Properties

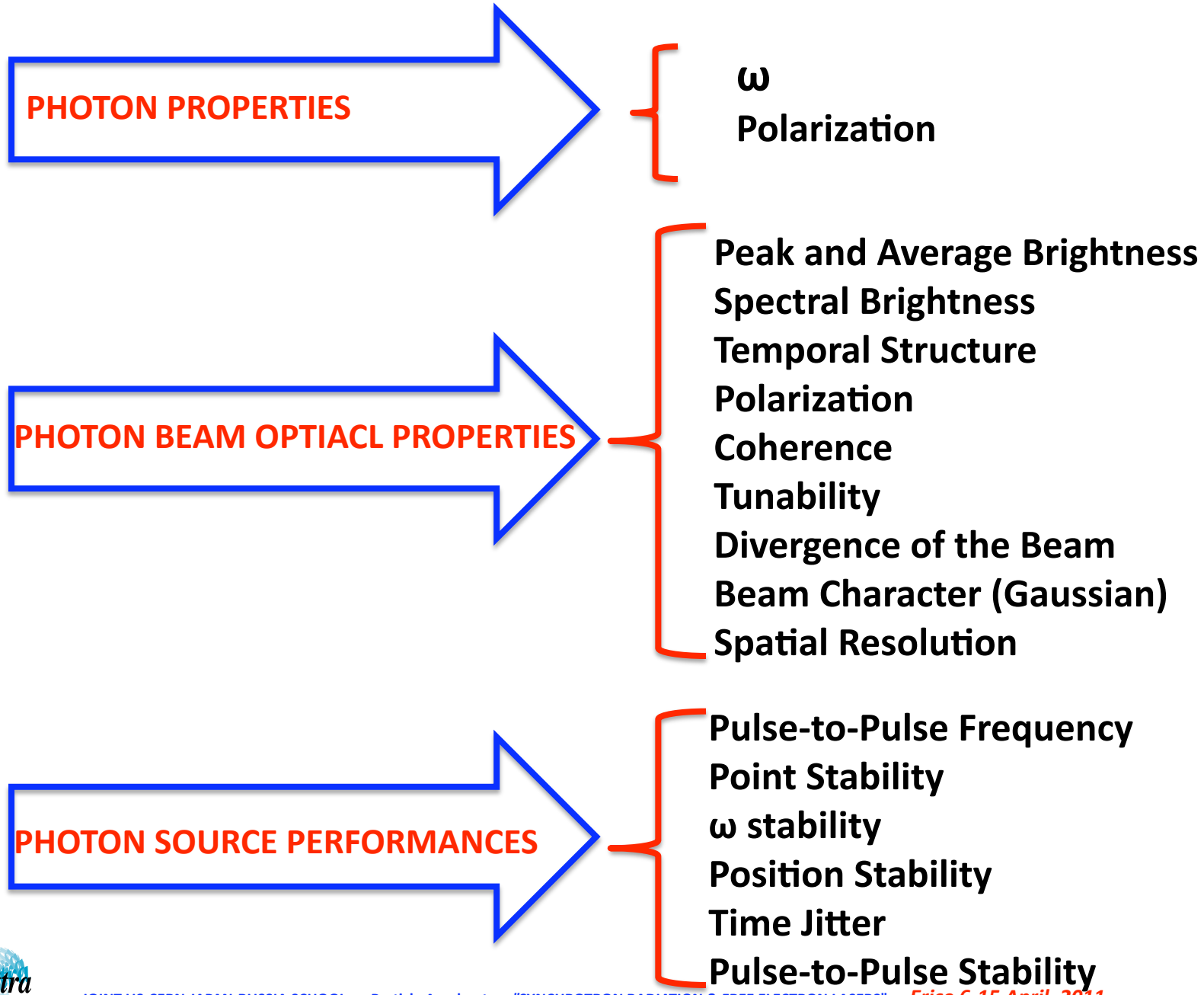

Source Parameters versus Experiments 1

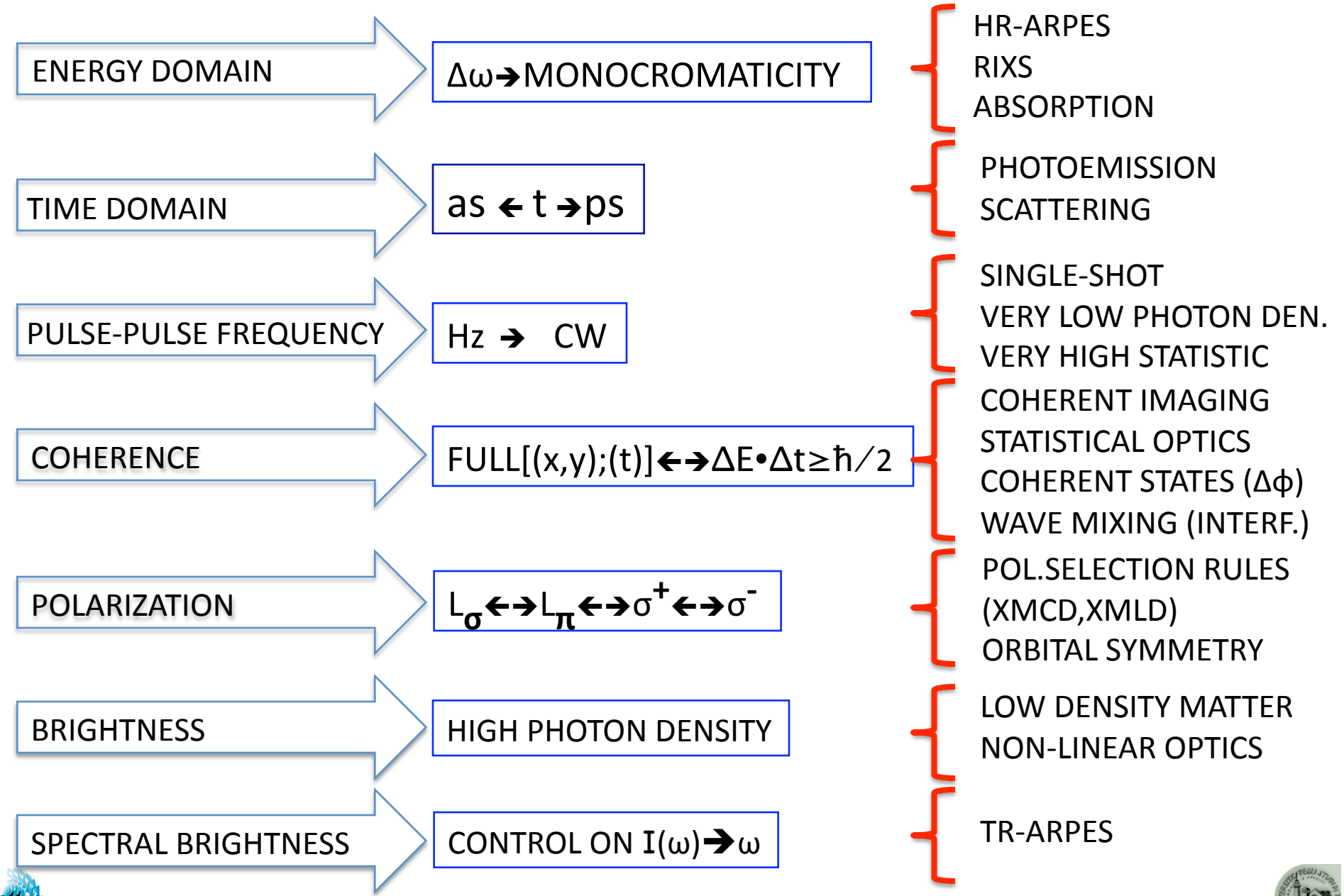

Source Parameters versus Experiments 2

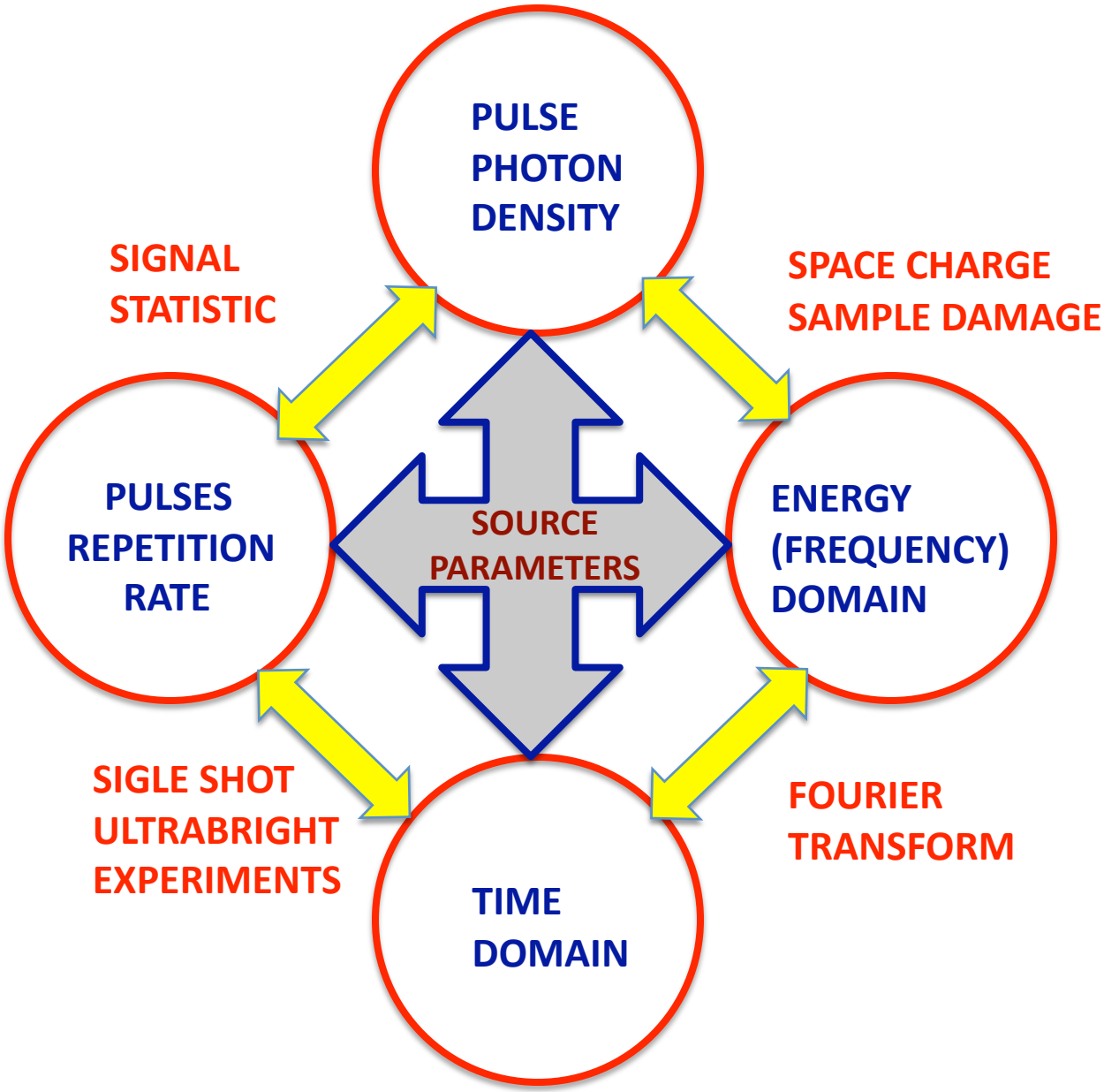

Future Light Sources 1

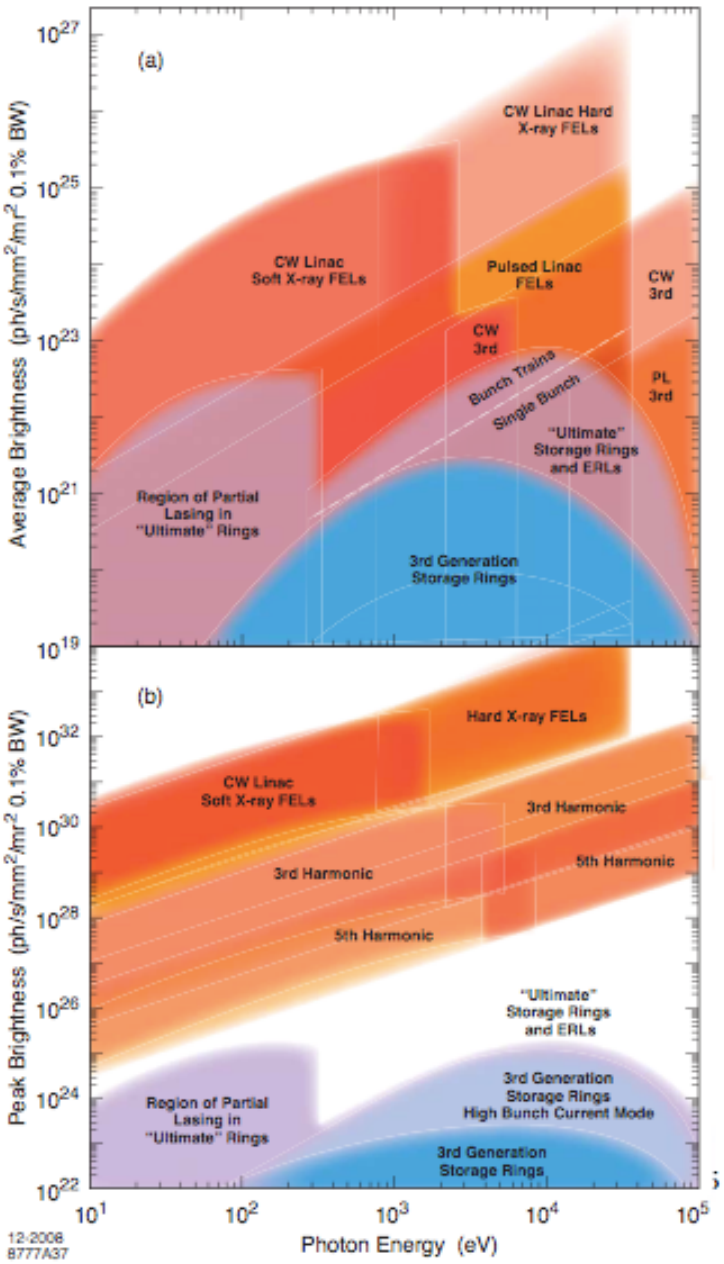

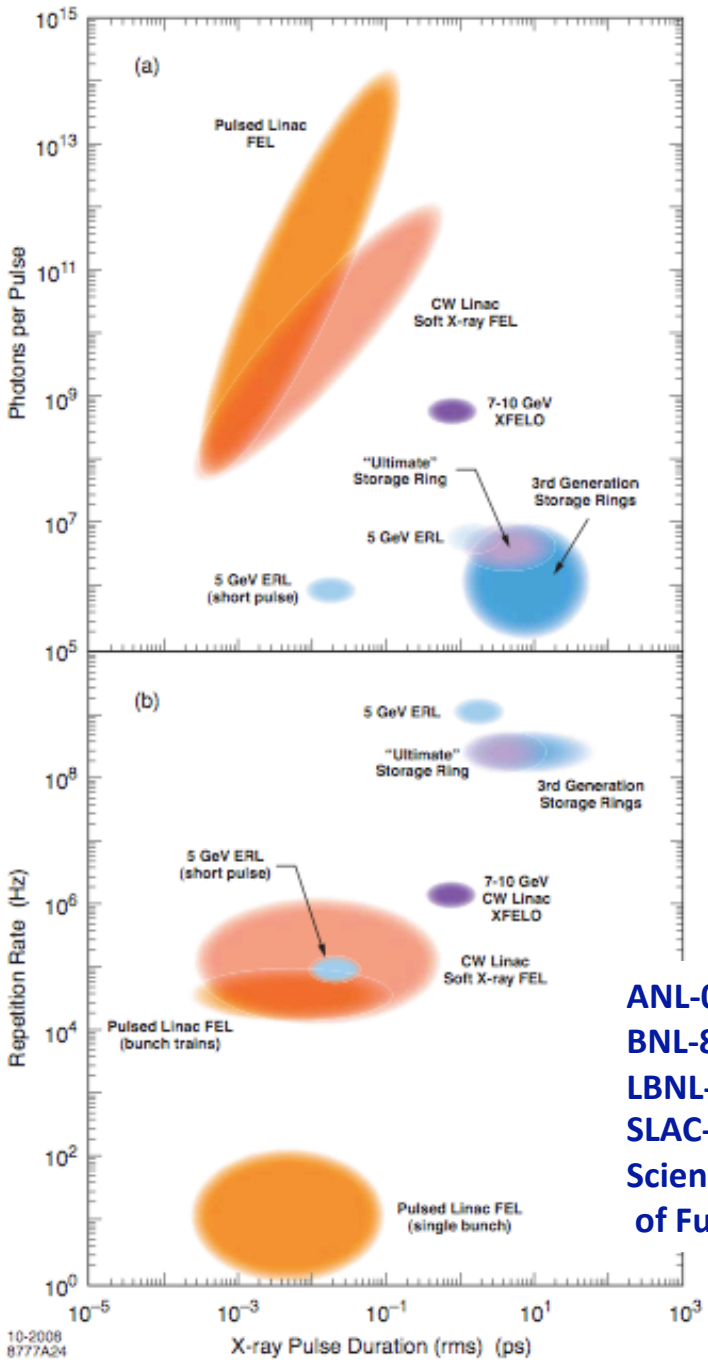

ANL-08/39
BNL-81895-2008
LBNL-1090E-2009
SLAC-R-917
Science and Technology of Future Light Sources

Future Light Sources 2

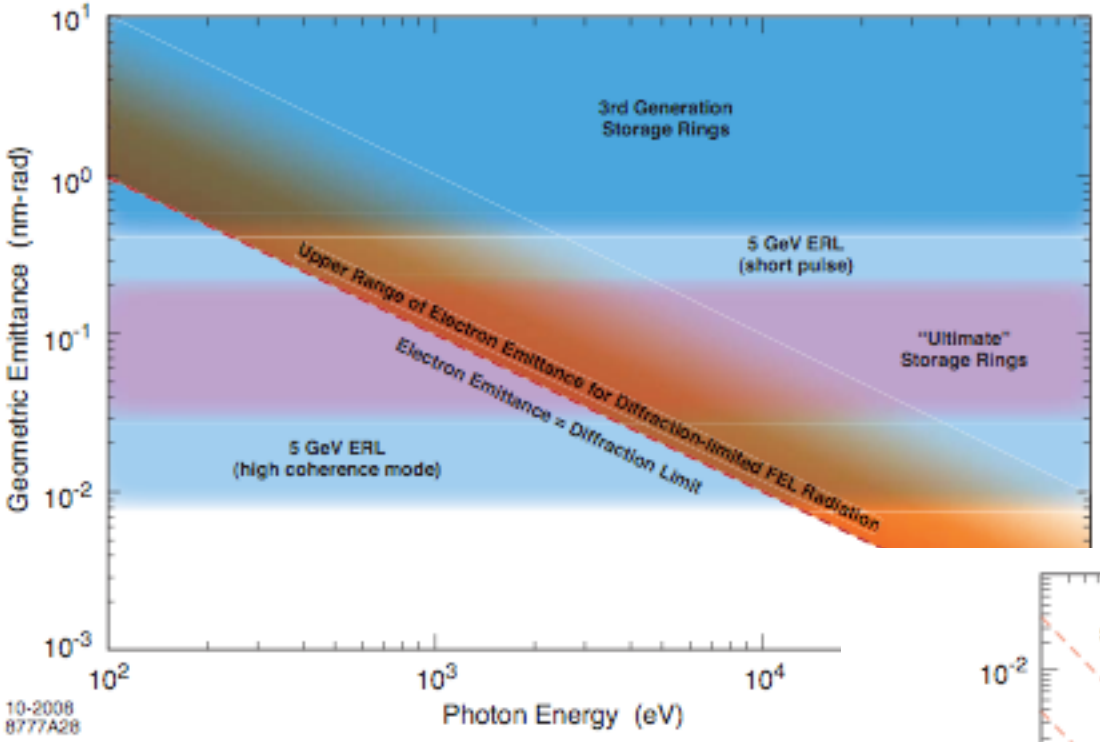

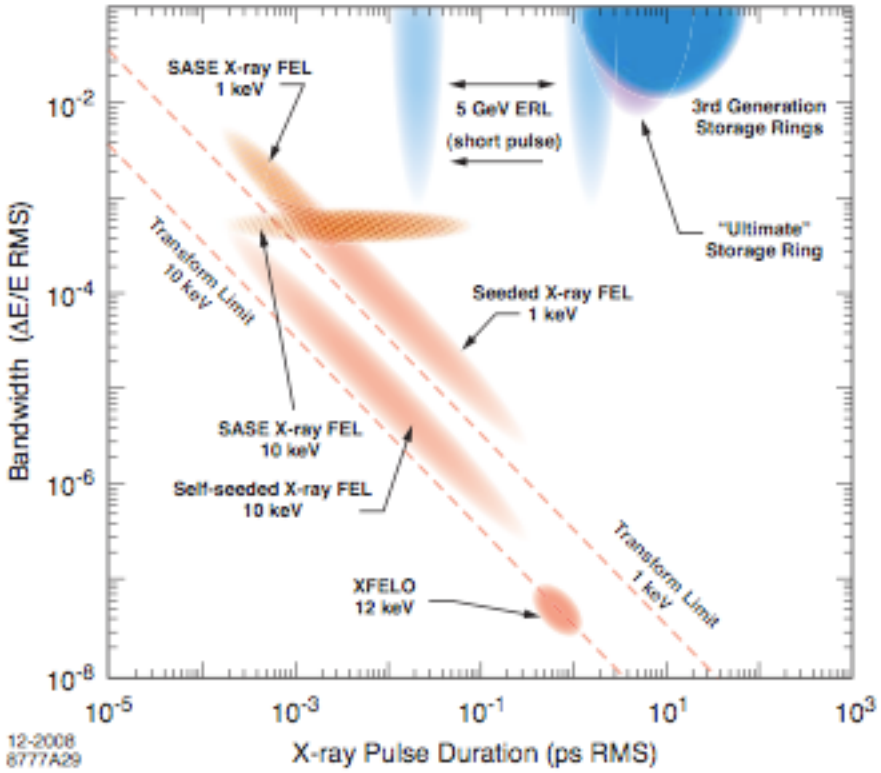

ANL-08/39
BNL-81895-2008
LBNL-1090E-2009
SLAC-R-917
Science and Technology of Future Light Sources

Conclusions

Frontier 1:
FELs
FULL COHERENCE ($\Delta E \bullet \Delta t \geq \hbar/2$)
ULTRASHORT TIME (as-fs)
ULTRABRIGHT

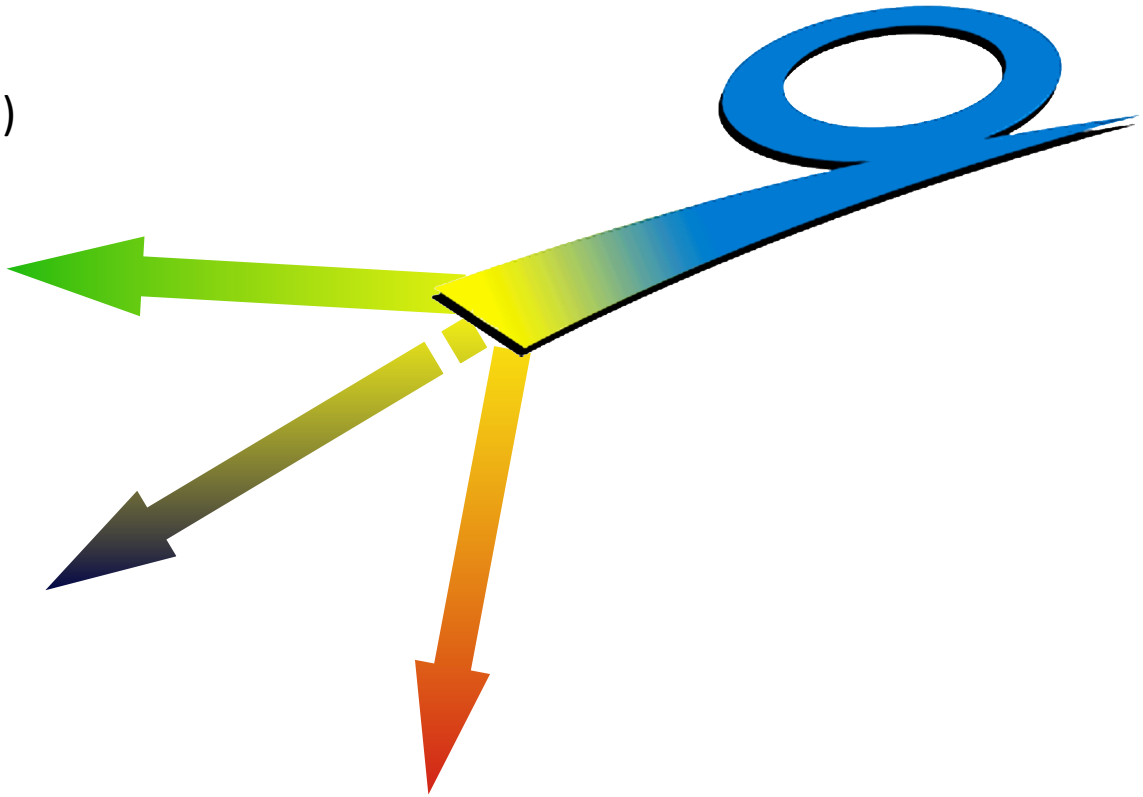

Frontier 2:
ERL AND ULTIMATE STORAGE RINGS
ENERGY DOMAIN EXPERIMENTS: (ω) (Δω, ΔQ),
HIGH RESOLUTION-HIGH STATISTICS
TIME RESOLVED (ps)

Frontier 3:
ACTUAL STORAGE RINGS
MOSTLY ANALYTICAL